

DESY 94-011  
WUB 94-04  
January 1994

## Beauty Physics in Lattice Gauge Theory

R. Sommer

Deutsches Elektronen-Synchrotron DESY, Hamburg

### Abstract

We summarize the present status of lattice gauge theory computations of the leptonic decay constants  $f_D$  and  $f_B$ . The various sources of systematic errors are explained in a manner easily understood by the non-expert. The results obtained by the different groups are then systematically compared. As a result, we derive estimates for  $f_D$  and  $f_B$  in the quenched approximation through an appropriate combination of the data available from the different groups. Since we account for a possible lattice spacing dependence, the final errors are quite large. However, it is now well known how these uncertainties can be reduced.

For the decay constant of heavy-light pseudoscalar mesons with masses of 1-2 GeV, an interesting comparison of a full QCD result with the corresponding simulation in the quenched approximation can be done. Effects of sea quarks of mass  $m_s$  are below the statistical accuracy of these simulations.

Related quantities, like  $B$ -parameters, the spectrum of beauty-hadrons and the breaking of the QCD string are discussed briefly.

# Contents

<b>1. Introduction</b>	<b>4</b>
<b>2. Lattice QCD</b>	<b>7</b>
2.1 Path Integral Representation of Greens Functions . . . . .	7
2.2 A Pseudoscalar Correlation Function . . . . .	9
2.3 The Continuum Limit . . . . .	10
2.4 Renormalization . . . . .	12
2.5 Reaching Asymptotics . . . . .	15
2.6 The Quenched Approximation . . . . .	19
2.7 The b-Quark on the Lattice . . . . .	24
<b>3. The Leptonic Decay Constants <math>f_D, f_{D_s}</math></b>	<b>27</b>
3.1 Extrapolation to Light Quark Masses . . . . .	28
3.2 Finite Size Effects . . . . .	28
3.3 Lattice Spacing Dependence and Renormalization . . . . .	30
3.4 Estimate in the Quenched Approximation . . . . .	34
3.5 Full QCD . . . . .	34
<b>4. The Leptonic Decay Constants <math>f_B, f_{B_s}</math></b>	<b>37</b>
4.1 Static Approximation . . . . .	37
4.2 Mass Dependence . . . . .	42
4.3 Interpolation . . . . .	44

4.4	Comparison to QCD Sum Rule Estimates . . . . .	45
4.5	Potential Improvements . . . . .	45
<b>5.</b>	<b>B-Parameter</b>	<b>47</b>
<b>6.</b>	<b>The Size of <math>1/m_h</math> Corrections to the Heavy Quark Limit</b>	<b>49</b>
<b>7.</b>	<b>The <math>B - \bar{B}</math> Threshold, String Breaking and Hybrid Mesons</b>	<b>50</b>
<b>8.</b>	<b>The Beauty Spectrum</b>	<b>54</b>
<b>9.</b>	<b>Further Lattice Investigations</b>	<b>57</b>
<b>10.</b>	<b>Summary</b>	<b>58</b>
<b>A</b>	<b>Renormalization of Vector Currents</b>	<b>59</b>
	<b>References</b>	<b>62</b>

# 1. Introduction

During the past decades, experiments in high energy physics have resulted in quite an in-depth understanding of the interactions between quarks and leptons. It is mathematically formulated as the Standard Model of particle physics. The fundamental parameters that characterize the overall strengths of the electromagnetic, weak and strong interactions in the Standard Model have been determined precisely in experiments. Also, the masses of the matter fields – apart from the postulated Higgs-boson and top-quark – are known. However, the detailed structure of the weak interactions of quarks is not determined well. Let us discuss this in more detail.

In the Standard Model, quark fields  $q$  couple to the charged weak interaction vector bosons  $W_+^\mu$  through a term

$$\sum_{U=u,c,t} \sum_{D=d,s,b} \bar{q}_U \gamma_\mu \frac{1 - \gamma_5}{2} V_{UD} q_D W_+^\mu .$$

The Cabibbo–Kobayashi–Maskawa (CKM) matrix[1]  $V_{UD}$  originates from the transformation from weak interaction eigenstates to mass eigenstates. Assuming that there are only three generations, it is unitary and can be written in terms of four observable parameters.

Given the strength of the weak interactions through  $\mu$  – decays, in principle one needs to determine the rate of decays of quarks such as  $d \rightarrow u$  to obtain the matrix elements of  $V$ . However, quarks do not exist as free particles and we can only observe the decay of hadrons. In general, the full knowledge of the hadron wave function is needed in order to relate a measured decay rate of a hadron to the parameter  $V_{UD}$  in the Lagrangian.

Fortunately, the neutron and the proton are related by isospin symmetry which is well tested experimentally. Hence, the vector part of the decay amplitude of the ordinary  $\beta$  decay ( $n \rightarrow p$ ) is given by a Clebsch–Gordan coefficient times the desired parameter. So  $|V_{ud}|$  can be determined with almost no theoretical input.

Analogously,  $|V_{us}|$  can be extracted from  $K \rightarrow \pi$  decays starting from an approximate  $SU(3)_{flavor}$  symmetry. Here, it is already important to include symmetry breaking corrections, which can be done reliably using chiral perturbation theory[2].

With these two matrix elements determined from experiment[3] (  $|V_{ud}| = 0.9744(10)$ ,  $|V_{us}| = 0.2205(18)$  ) and imposing the constraints of unitarity, Wolfenstein observed that mixing appears hierarchically[4]. The hierarchy is parametrized by a small pa-

parameter  $\lambda = |V_{us}|$ :

$$V = \begin{pmatrix} V_{ud} & V_{us} & V_{ub} \\ V_{cd} & V_{cs} & V_{cb} \\ V_{td} & V_{ts} & V_{tb} \end{pmatrix} = \begin{pmatrix} 1 - \lambda^2/2 & \lambda & A\lambda^3(\rho - i\eta) \\ -\lambda & 1 - \lambda^2/2 - iA^2\lambda^4\eta & A\lambda^2 \\ A\lambda^3(1 - \rho - i\eta) & -A\lambda^2 & 1 \end{pmatrix}.$$

The other parameters  $A, \rho$  and  $\eta$  are of order  $O(\lambda^0)$ .

The parameter  $A$  has been determined from semileptonic decays  $B \rightarrow D^* l \nu$ . As theoretical input, one needs some information on the formfactors of these transitions. This has previously been extracted using model wave functions for the  $B^-$  and the  $D^-$ -mesons [5]. It has been discovered, however, that the theoretical description of these formfactors is considerably simplified in the limit when the masses of both the  $b$  and the  $c$  quark are large compared to typical hadronic scales. In this limit, there appears an approximate  $SU(2)_{flavor} \times SU(2)_{spin}$  symmetry relating the  $b$ -quark and the  $c$ -quark. Consequently, the number of formfactors describing these transitions is reduced to one, the Isgur–Wise function[6]. The effective theory that starts from this symmetry and tries to include the corrections of order  $O(m_N/m_h)$ , with  $m_h$  the heavy quark mass and  $m_N$  the nucleon mass representing a typical QCD scale, as well as the QCD radiative corrections, is called Heavy Quark Effective Theory (HQET). Apart from radiative corrections[7], the normalization of the Isgur–Wise function at the point  $v \cdot v' = 1$  ( $v$  and  $v'$  are the 4-velocities of the initial and final state meson respectively) is given by the symmetry up to corrections of order  $O((m_N/m_c)^2)$  [9]. Assuming that the latter terms are small, one extrapolates the experimental data to that kinematical point and one obtains[10, 11]  $A = 0.90(12)$ .

Again, a symmetry has helped to circumvent the full solution of the bound state problem of QCD. It is important to note, however, that in the case of the HQET, we have to date a far more limited understanding of the size of symmetry breaking terms than in the case of  $SU(3)_{flavor}$ . In the latter case, there is a large amount of experimental information on symmetry breaking, which helped to develop a comprehensive theoretical treatment of these effects. Therefore, it is of interest to quantify or bound the  $O((m_p/m_c)^2)$  corrections in the above analysis. A promising approach to this problem are lattice gauge theory calculations of the semileptonic form factors[12, 13]. In addition, QCD–sumrules allow to estimate the size of the  $O((m_p/m_c)^2)$  corrections[14].

There are two additional unknowns in the CKM-matrix:  $\rho$  and  $\eta$ . They are of particular interest, since they are a (and probably *the*) source of CP–violation in the Standard Model[15]. Their values are mainly constrained by three experimental observations.

$B$ -meson decays together with model calculations determine [11]  $\sqrt{\rho^2 + \eta^2} = 0.36(9)$ . Moreover, the CP–violation parameter  $|\epsilon|$  in the  $K$ -system[15] and the  $B_0$ – $\bar{B}_0$  mixing parameter  $x_d$  restrict  $\rho$  and  $\eta$ . However, in order to extract  $\rho$  and  $\eta$  from these

measurements, one needs to know the mixing matrix elements

$$\frac{8}{3}B_B f_B^2 M_B^2 = \langle B_0 | (\bar{d}\gamma_\mu(1 - \gamma_5)b)(\bar{d}\gamma_\mu(1 - \gamma_5)b) | \bar{B}_0 \rangle$$

and

$$\frac{8}{3}B_K f_K^2 M_K^2 = \langle K_0 | (\bar{d}\gamma_\mu(1 - \gamma_5)s)(\bar{d}\gamma_\mu(1 - \gamma_5)s) | \bar{K}_0 \rangle \quad ,$$

where  $f_B$  and  $f_K$  are the leptonic decay constants of the  $B^-$  and the  $K^-$ -mesons and  $B_B$ ,  $B_K$  parametrize the matrix elements relative to the vacuum insertion “approximation” [15].

The dependence of the allowed domain in the  $(\rho, \eta)$  plane on the theoretical uncertainty of  $B_K$  ( $f_K$  is known from experiment) is not very large. The allowed region depends sensitively on the value of the product  $B_B f_B^2$ , however [16, 17, 11].

Until fairly recently, phenomenological analysis of the allowed region in the  $(\rho, \eta)$  plane used the “old prejudice”  $f_B \sqrt{B_B} = (110 - 160)$  MeV. Such values favor a negative  $\rho$  and lead to small predictions of CP-asymmetries in  $B$  decays, which one would like to measure in future experiments at  $B$ -factories [8]. First lattice estimates [18, 19] of these quantities that were done within the HQET approximation, indicated much larger values of  $f_B$ . Also, QCD sum rule calculations performed in the HQET limit have subsequently yielded such large values [20, 21]. Together with  $B_B \simeq 1$  which is supported by a number of theoretical investigations, this indicates that positive values of  $\rho$  are favored by the experimental constraints. If this is the case, much larger signals for CP-violation in  $B$  decays are expected – an interesting perspective for  $B$ -factories.

We emphasize, that the value of  $B_B f_B^2$  is the central theoretical uncertainty on our way from the experimental data to the determination of the CP-violating part of the CKM-matrix. It is therefore important to determine  $B_B f_B^2$  with a good precision in order to narrow down the allowed region of  $(\rho, \eta)$ . To this end, precise lattice calculations of these quantities are necessary and one has to take account of the full spectrum of the statistical *and* systematic uncertainties. Besides this number (and similar other ones that are of interest), lattice gauge theory calculations also offer the possibility to quantify the corrections to the HQET limit. Starting from the simpler case of the  $D$ -meson, we review the present status of these efforts and their future perspective in sections 4., 5. and 6.. A discussion of some general features of lattice gauge theory calculations – as given in section 2. – is needed to understand the different sources of systematic errors in the computations. Other sections cover related topics.

## 2. Lattice QCD

Lattice QCD[22, 23] is a regularization of the fundamental theory of strong interactions that allows nonperturbative calculations. In principle, it involves no approximations. The latter arise because our numerical possibilities of evaluating the path integral by a Monte Carlo process are limited. This means that computations have to be performed at parameters that are different from their values in nature. Therefore, extrapolations have to be performed e.g. in the lattice spacing, quark masses and the space-time - volume  $V$ . Furthermore, we are limited by the statistical errors of the Monte Carlo calculation.

In order to be able to discuss the various systematic errors in current calculations, we need to introduce some definitions and summarize the crucial points in a practical lattice QCD computation. This section primarily addresses readers that are not very familiar with lattice QCD. The specialist may, however, be interested in the discussion about universality in the quenched approximation, which is given in section 2.6.

### 2.1 Path Integral Representation of Greens Functions

The starting point of lattice QCD is to define the field theory on a space-time lattice with spacing  $a$ . This is one way of regularizing the ultraviolet divergences that are intrinsic to a quantum field theory: the lattice spacing serves as a cutoff for the high frequency modes of the fields. As in the case of any cutoff, the field theory is finally defined in the limit  $a^{-1} \rightarrow \infty$ .

The basic variables of lattice QCD are the dimensionless quark fields  $q_f(x)$  ( $f$  labels the different flavors of quarks and we omit the color- and Dirac-indices) and the gluon field variables  $U_\mu(x)$  which are  $SU(3)$  matrices. The coordinate  $x$  resides on the 4-dimensional space-time lattice:  $x = (x_0, x_1, x_2, x_3)$ ,  $x_\mu/a \in N$ . The gluon variables  $U_\mu(x)$  are the gauge connection of nearest neighbor points  $x$  and  $x + a\hat{\mu}$ .

The dynamics of the theory (i.e. bound state masses and properties, transition probabilities) is contained in the euclidean Greens functions or correlation functions. They are defined through the Feynman path integral

$$\begin{aligned} \langle O[q, \bar{q}, U] \rangle &= Z^{-1} \int D[q] \int D[\bar{q}] \int D[U] \exp(-S[q, \bar{q}, U]) O[q, \bar{q}, U] \\ Z &= \int D[q] \int D[\bar{q}] \int D[U] \exp(-S[q, \bar{q}, U]). \end{aligned} \quad (2.1)$$

Here,  $\int D[q] \int D[\bar{q}]$  stand for multiple Grassmann integrals over each component of the quark variables and  $\int D[U]$  represents an integral over the gluon variables on each link

with the SU(3) Haar measure.  $O[q, \bar{q}, U]$  is a functional of any number of variables of the theory and  $S[q, \bar{q}, U]$  is the euclidean action

$$S[q, \bar{q}, U] = S_G[U] + S_F[q, \bar{q}, U] \quad (2.2)$$

with a gluonic part

$$S_G[U] = \beta \sum_x \sum_{\mu > \nu = 0}^3 \left\{ 1 - \frac{1}{6} \text{Re tr } P_{\mu, \nu}(x) \right\}; \quad \beta = \frac{6}{g_0^2} \quad (2.3)$$

and a fermionic part

$$S_F[\bar{q}, q, U] = \sum_x \bar{q}(x) \mathcal{D} q(x); \quad (2.4)$$

$$\mathcal{D} = M_0 + \frac{1}{2} \left[ \sum_{\mu=0}^3 \gamma_\mu (\nabla_\mu + \nabla_\mu^*) - \sum_{\mu=0}^3 \nabla_\mu \nabla_\mu^* + i \frac{c_{SW}(g_0^2)}{2} \sum_{\mu, \nu=0}^3 F_{\mu\nu} \sigma_{\mu\nu} \right].$$

Here,  $P_{\mu, \nu}(x)$  is the product of gauge parallel transporters  $U_\mu(x)$  around an elementary plaquette

$$P_{\mu, \nu}(x) = U_\mu(x) U_\nu(x + a\hat{\mu}) U_{-\mu}(x + a\hat{\mu} + a\hat{\nu}) U_{-\nu}(x + a\hat{\nu}); \quad U_{-\mu}(x) \equiv U_\mu^\dagger(x - a\hat{\mu}), \quad (2.5)$$

the covariant finite differences are

$$\nabla_\mu q(x) = U_\mu(x) q(x + a\hat{\mu}) - q(x), \quad \nabla_\mu^* = -\nabla_{-\mu} \quad (2.6)$$

and the euclidean gamma matrices fulfill

$$\{\gamma_\mu, \gamma_\nu\} = 2\delta_{\mu, \nu}, \quad \gamma_\mu^\dagger = \gamma_\mu, \quad \sigma_{\mu\nu} = \frac{i}{2} [\gamma_\mu, \gamma_\nu]. \quad (2.7)$$

A lattice approximation of the field strength is given by

$$F_{\mu\nu}(x) = \frac{1}{8} \left[ P_{\mu, \nu}(x) + P_{-\mu, -\nu}(x) + P_{\nu, -\mu}(x) + P_{-\nu, \mu}(x) \right. \\ \left. - P_{\nu, \mu}(x) - P_{-\nu, -\mu}(x) - P_{-\mu, \nu}(x) - P_{\mu, -\nu}(x) \right]. \quad (2.8)$$

The lattice action  $S$  depends on the bare parameters of the theory, namely  $g_0^2$ , the gauge coupling, and the hopping parameters  $K_f$  that are collected in the bare quark mass matrix  $M_0 = \text{diag}(1/(2K_1), \dots, 1/(2K_{n_f})) - 4$ . The last term in the fermion matrix[24]  $\mathcal{D}$ , which is accompanied by the coefficient function  $c_{SW}(g_0^2)$  will be discussed at the end of section 2.3.

Eq. (2.1) looks identical to a statistical mechanics thermal average. It can be evaluated by Monte Carlo importance sampling, once the space time grid is restricted to a finite number of points[23]. Such a Monte Carlo evaluation is the main nonperturbative method employed in lattice gauge theory calculations. There is an essential difference



to a simulation of a spin model, however, namely the fermionic nature of the quark fields. Since the fermionic action is a quadratic form, the Grassmann integrals can be performed analytically, e.g.

$$\int D[q] \int D[\bar{q}] q_{\alpha'}^c(x') \bar{q}_{\alpha}^c(x) = \mathcal{D}_{x,f,\alpha,c;x',f',\alpha',c'}^{-1}[U] \det \mathcal{D}[U] \exp(-S_G[U]) , \quad (2.9)$$

with  $\alpha, \alpha'$  Dirac indices and  $c, c'$  color indices. In general, one obtains

$$\langle O[q, \bar{q}, U] \rangle = Z^{-1} \int D[U] \exp(-S_G[U]) \det \mathcal{D}[U] F_O[U] \quad (2.10)$$

with a functional  $F_O[U]$  that is easily derived using eq. (2.9) and the property that the Grassmann fields are anticommuting. It is eq.(2.10) which is evaluated by Monte Carlo important sampling, generating “configurations”  $U$  with the probability  $P[U] \propto \exp(-S_G[U]) \det \mathcal{D}[U]$  and then averaging  $F_O[U]$  over these configurations.

## 2.2 A Pseudoscalar Correlation Function

We discuss here the most simple (and for the purpose of this review almost sufficient) observable that is well calculable in lattice QCD. We choose a lattice with a finite number of points  $L/a$  in the three space directions and  $L_t/a$  points in euclidean time. The gauge fields are periodic functions:  $U_{\mu}(x) = U_{\mu}(x + \hat{k}L)$ ,  $k = 1, 2, 3$ ;  $U_{\mu}(x) = U_{\mu}(x + \hat{0}L_t)$ . The quark fields are taken antiperiodic in time and periodic (or antiperiodic) in space. We may take the axial vector current

$$A_{\mu}^{ff'}(x) = Z_A \bar{q}_f(x) \gamma_{\mu} \gamma_5 q_{f'}(x) \quad (2.11)$$

as a convenient interpolating field for pseudoscalar mesons<sup>1</sup>:

$$\langle 0 | A_0(0) | P \rangle = F_P \sqrt{M_P/2} . \quad (2.12)$$

The finite renormalization  $Z_A$  of the axial vector current will be discussed in section 2.4. The (space-) momentum zero correlation function of  $A_0$  has a spectral decomposition

$$\sum_{\vec{x}} \langle A_0(x) A_0^{\dagger}(0) \rangle = \sum_{n \geq 1} | \langle 0 | A_0 | P, n \rangle |^2 \{ \exp[-E_n x_0] + \exp[E_n(x_0 - L_t)] \} , \quad (2.13)$$

where  $|P, n \rangle$  denote the excited states in this channel and  $|P, 1 \rangle \equiv |P \rangle$ .

With the Wilson action (i.e.  $c_{SW}(g_0^2) \equiv 0$ ), the transfer matrix, which describes the propagation in the euclidean time, is positive and hermitian[25]. In this case, eq. (2.13) is therefore exact up to irrelevant terms of order  $O(\exp[-E_{gap}L_t])$ , where  $E_{gap}$  is the

---

<sup>1</sup>  $|P \rangle$  denotes the pseudoscalar state with momentum zero, the appropriate flavor quantum numbers and with a normalization  $\langle P | P \rangle = 1$ .

lowest state with the quantum numbers of the vacuum. When  $c_{SW}(g_0^2) \neq 0$ , one expects eq. (2.13) to hold to a good approximation at moderately large  $x_0$ .

At sufficiently large values of the euclidean time  $x_0$ , the spectral representation shows that the correlation function eq. (2.13) is dominated by the lowest state and one may extract both the mass  $M_P \equiv E_1$  and the leptonic decay constant  $F_P$  from a Monte Carlo estimate of  $\langle A_0(x)A_0^\dagger(0) \rangle$ .

### 2.3 The Continuum Limit

In this section, we discuss how the continuum limit  $a \rightarrow 0$  is taken in QCD.

Lattice gauge theories contain only dimensionless variables and fields. All quantities are calculated in units of the lattice spacing  $a$ . The latter is not a parameter of the calculation but is determined a posteriori once a dimensionful observable is fixed to its experimental value.

In order to shorten the discussion, consider QCD with only mass-degenerate quarks, i.e.  $K_f = K$  for all  $f$ . Eq. (2.13) then determines the dimensionless functions<sup>2</sup>

$$F_P(g_0^2, K) \tag{2.14}$$

and

$$M_P(g_0^2, K) . \tag{2.15}$$

In addition, for example, the mass of the nucleon in lattice units  $M_N(g_0^2, K)$  may be calculated from a nucleon correlation function.

Since the quark masses are free parameters in the Standard Model, we have to set a nonperturbative renormalization condition to fix the hopping parameter  $K$  in terms of a renormalized, experimentally observable quantity. A convenient choice is

$$M_P(g_0^2, K)/F_P(g_0^2, K) = m_\pi/f_\pi , \tag{2.16}$$

where  $f_\pi$  and  $m_\pi$  refer to the experimentally measured leptonic decay constant and mass of the pion. Eq. (2.16) defines a renormalization group trajectory in the  $(g_0^2, K)$  plane. Along this trajectory, the ratio

$$R_{M_N, F_P}(F_P) \equiv \frac{M_N(g_0^2, K)}{F_P(g_0^2, K)} \Big|_{M_P(g_0^2, K)/F_P(g_0^2, K) = m_\pi/f_\pi} \tag{2.17}$$

---

<sup>2</sup> We assume that at each point  $(g_0^2, K)$ , the space extent  $L$  of the lattice has been chosen large enough such that finite size effects are negligible compared to the statistical accuracy of the calculation. Therefore, the dependence on the third dimensionless parameter  $(F_P L/a)$  is not written.

is a function of  $F_P$  only and reaches its continuum limit at  $F_P = 0$  since  $F_P$  is the physical decay constant times the lattice spacing. From asymptotic freedom one infers that the continuum limit is reached at the point  $g_0^2 = 0$ ,  $K = 1/8$ .

Equivalently, on the trajectory eq. (2.16), we may consider the lattice spacing to be determined by

$$a_{f_\pi}(g_0^2) = F_P(g_0^2, K)/f_\pi \quad (2.18)$$

and the nucleon mass in physical units is given by  $m_N = M_N(g_0^2, K)/a_{f_\pi}(g_0^2)$ .

Corrections to the continuum limit constitute a major source of uncertainty for practical lattice gauge theory determinations of quantities like  $f_B$ . These corrections have to be addressed by Monte Carlo simulations done at different points on the renormalization group trajectory. Nevertheless, it is instructive to consider perturbation theory and learn something about the *structure* of the finite lattice spacing corrections. Symanzik has discussed the cutoff dependence of Feynman diagrams[26]. For the action eq. (2.4), such a discussion[24] suggests that the leading dependence of physical quantities such as  $R_{M_N, F_P}(F_P)$  on the lattice spacing is linear (up to numerically unimportant logarithmic modifications):

$$R_{M_N, F_P}(F_P) = \frac{m_N}{f_\pi} + \rho_1 F_P + O(F_P^2) ; \quad F_P \equiv f_\pi a_{f_\pi} . \quad (2.19)$$

How small does the lattice spacing have to be such that the finite  $a$  corrections are small? Again this can only be answered by a nonperturbative calculation of the function  $R_{M_N, F_P}(F_P)$  and for each such a function separately. It is however worth noting, that one may expect that the relevant scales are the sizes of the wave functions of the hadrons considered (for S-wave states), not their Compton wave length, since we mainly need a good approximation of the continuum wave function by the lattice one. We may therefore hope that eq. (2.19) can be applied for  $a \ll 0.5 fm$ .

### Improving the Approach to the Continuum Limit

In a formal expansion in powers of the lattice spacing, the fermion action eq. (2.4) breaks up into three pieces. The first two, the naively discretized Dirac operator and the Wilson term, are necessary to obtain the correct continuum limit[27]. The Wilson term,  $\bar{q} \sum_\mu \nabla_\mu \nabla_\mu^* q$  has a classical continuum limit  $-a\bar{q}\Delta q + O(a^2)$ , where  $\Delta$  is the covariant Laplace operator. This dimension 5, irrelevant, operator is responsible for the lattice spacing corrections of order  $O(a)$  as e.g. in eq. (2.19). It is expected that for *on-shell* matrix elements these terms can be cancelled by adding *one* dimension 5 operator to the action[28]. Most conveniently, one chooses the third term in the action with coefficient function  $c_{SW}(g_0^2)$ , since it does not involve further derivative terms in the quark fields[24].

Symanzik's idea was to calculate coefficients like  $c_{SW}(g_0^2)$  in perturbation theory leading to a perturbatively improved action. Already the tree level expression  $c_{SW}(g_0^2) = 1$

leads to  $\rho_1 = O(g_0^2)$ . Since i) the arguments that lead us to expect that the  $O(a)$  lattice artifacts can be cancelled in this way are due to perturbation theory and ii) the coefficient function  $c_{SW}(g_0^2)$  is calculated perturbatively, improvement needs to be demonstrated through Monte Carlo results. At present, the evidence for improvement with the action of Sheikholeslami and Wohlert is somewhat indirect but nevertheless suggests that  $O(a)$  lattice artifacts are significantly reduced compared to the Wilson action[29]. In this context, it is furthermore of interest that in the case of the pure gauge theory with Dirichlet boundary conditions, an improvement has been established unambiguously for a one loop Symanzik improved action[30]. Thus, there is an example which shows that the perturbative improvement program of Symanzik works at those values of the gauge coupling that are needed in realistic simulations.

Below, we will also discuss recent results for heavy-light (HL) mesons that were obtained with the perturbatively improved action. We will use the synonyms “improved action” and “SW-action” for the action eq. (2.4) with  $c_{SW}(g_0^2) = 1$ , while we use the name “Wilson action” when  $c_{SW}(g_0^2) = 0$ .

## 2.4 Renormalization

In the previous section, we have ignored the problem of the determination of the strength of the axial vector current  $Z_A$ . At first sight, it requires a nontrivial renormalization since it is a composite operator. However, at the formal level, the flavor offdiagonal axial vector current  $A_\mu^{f,f'}(x)$  is the current of chiral symmetry, which is broken only softly:

$$\partial_\mu A_\mu^{f,f'}(x) = (m_f + m_{f'}) P^{f,f'}(x); \quad P^{f,f'}(x) = \bar{q}_f(x)\gamma_5 q_{f'}(x) . \quad (2.20)$$

This relation (more precisely the chiral ward identities) would normally insure that  $A_\mu$  does not get renormalized. The quantum field theory needs to be defined with a regulator, however. As the lattice regularization (eq. (2.4)) breaks chiral symmetry by terms of order  $O(a)$ , the formal argument does not apply and  $A_\mu$  acquires a nontrivial renormalization[31, 32].<sup>3</sup>

In the following, we mainly discuss the case of the Wilson action, which is still the action for which most results exist. At the very end of this section, we mention the case  $c_{SW} = 1$ .

We write the relation between the bare lattice current and the renormalized current  $A_\mu^{f,f'}(x)$  in the most general way:

$$A_\mu^{f,f'}(x) = Z_A(g_0^2, K_f, K_{f'}) \bar{q}_f(x)\gamma_\mu\gamma_5 q_{f'}(x) . \quad (2.21)$$

---

<sup>3</sup> Only in the case of the vector current, a conserved current can be defined for most actions.

Here,  $Z_A$  needs to be defined through an appropriate normalization condition, such as eq.(2.27) which will be discussed below. We may rewrite eq. (2.21) in a form that was suggested by Lepage, Kronfeld and Mackenzie[33, 34, 35]<sup>4</sup>

$$A_\mu^{f,f'}(x) = \tilde{Z}_A(g_0^2, K_f, K_{f'}) \sqrt{\frac{1}{2K_f} - 3\bar{u}} \sqrt{\frac{1}{2K_{f'}} - 3\bar{u}} \bar{q}_f(x) \gamma_\mu \gamma_5 q_{f'}(x) , \quad (2.22)$$

where the mean field value  $\bar{u}$  of the gauge field is defined through a gauge invariant quantity, e.g.[34]

$$\bar{u} = 1/(8K_{crit}) . \quad (2.23)$$

The critical value of the hopping parameter  $K_{crit}$  is to be determined nonperturbatively from the Monte Carlo calculations through  $M_P(g_0^2, K_{crit}) = 0$ .

If the renormalization constants  $Z_A$  and  $\tilde{Z}_A$  are defined through a nonperturbative normalization condition at a finite value of the lattice spacing, eq's. (2.21,2.22) are completely equivalent. In most applications, the normalization of the currents is taken from perturbation theory and after dropping the  $O(a)$  terms. In this approximation, there is a significant difference between the currents (2.21,2.22). Numerically, the difference is dominated by a factor  $\exp[(m_f + m_{f'})a/2]$ ;  $am_f \equiv \log[1 + (2K_f)^{-1} - (2K_{crit})^{-1}]$ . Although this factor becomes irrelevant in the continuum limit, it is sizeable in present HL calculations.

In 1-loop order perturbation theory one obtains[31, 36, 35]

$$Z_A(g_0^2, K_f, K_{f'}) = 1 - 0.133373\tilde{g}^2 + O(\tilde{g}^4) + O(am_f) + O(am_{f'}) \quad (2.24)$$

$$\tilde{Z}_A(g_0^2, K_f, K_{f'}) = 1 - 0.02480 \tilde{g}^2 + O(\tilde{g}^4) + O(am_f) + O(am_{f'}) \quad (2.25)$$

$$\tilde{g}^2 = g_0^2/P ; \quad P = \frac{1}{3} < \text{tr} P_{\mu,\nu}(x) > . \quad (2.26)$$

In the above equations, we did not need to specify the normalization condition for the current, because the  $Z$ -factors depend on these conditions only when  $O(am_f)$ -terms are included. Instead of using the bare coupling as expansion parameter, we have written the perturbative expansion of  $Z_A, \tilde{Z}_A$  in terms of the effective coupling  $\tilde{g}^2$ , introduced by G. Parisi[39]. Through several examples, Lepage and Mackenzie[37, 35] demonstrated that the series in  $\tilde{g}^2$  (at momentum scales of the lattice cutoff  $\pi/a$ )

---

<sup>4</sup> The argument that is given in ref. [33] for this normalization is based on the limit  $am_f \gg 1$  and is therefore only indicative in the present context. On the other hand, Kronfeld[34] starts from the canonical normalization of the quark fields in the transfer matrix representation[25] of Green functions like eq. (2.13). Subsequently, he uses a mean field approximation *and implicitly assumes* that the quark fields enter with zero space-momentum. One is therefore well advised to consider this normalization as an alternative and not as the solution to the problem of handling heavy quarks with masses of the order of the inverse lattice spacing.

converges more rapidly than the one in the bare coupling<sup>5</sup>. In the known examples, the correction terms to the 1-loop order are compatible with having coefficients of the order one or less, when the series is written in terms of  $\tilde{\alpha} = \tilde{g}^2/(4\pi)$ . In addition, Lepage and Mackenzie present examples where 1-loop perturbation theory gives quite accurate results when compared to full nonperturbative computations of the quantity considered; see also ref. [38].

It is argued in ref. [34] that eq. (2.22) is the definition with the smaller lattice artifacts when it is used together with the perturbative value of the renormalization constant (as given above). In subsequent works, this normalization is quoted as the “correct” one and eq. (2.22) as “false”. We stress that this is not the case as a general statement and give a counter example in the appendix. The example, as well as the lattice spacing dependence of  $f_D$ , which we investigate later, mainly teaches us that the size of the lattice artifacts has to be determined by precise simulations with varying lattice spacings for each case separately (A one-loop calculation including the  $O(m_f a)$ -terms could shed some light onto this question as well).

The  $O(\tilde{g}^4)$  corrections to the one loop estimates of the renormalization constants are a systematic error. In principle, the axial current may be renormalized nonperturbatively. Here we only outline the idea and refer the reader to ref. [32] for a more detailed discussion. The idea is to require current algebra relations to be valid for the renormalized currents. For instance, one may require[32]

$$\begin{aligned} \frac{1}{2} \sum_x \langle [(m_f P^{f,f}(x) - \partial_\mu A_\mu^{f,f}(x)) - (f \rightarrow f')] A_\nu^{f,f'}(y) V_\nu^{f',f}(z) \rangle = \\ = -\langle V_\nu^{f,f'}(y) V_\nu^{f',f}(z) \rangle + \langle A_\nu^{f,f'}(y) A_\nu^{f',f}(z) \rangle \end{aligned} \quad (2.27)$$

for the renormalized currents. Taking  $\nu$  to be i) spacelike and ii) timelike, Eq.(2.27) constitutes two rather independent linear equations for the current renormalization constants. As these equations are nonlinear, the renormalization constants can be computed – without the use of perturbation theory.

It is important to note the following points about this equation<sup>6</sup>. The axial vector current at point  $y$  on the left hand side is changed into the vector current on the right hand side by the contact with the pseudoscalar density and analogously for  $V(z)$ . This means that the relevant contributions in the integrated three-point function on the

---

<sup>5</sup> Lepage and Mackenzie actually go further[35] and change from  $\tilde{g}^2$  to a physical coupling defined from the interquark potential. In addition, they give a prescription how to optimize the scale at which this coupling should be evaluated when one inserts it into a 1-loop perturbative result. Although this does indeed improve the agreement of 1-loop perturbation theory with nonperturbative Monte Carlo results for the examples that are considered in [35], it is important to be aware that the errors remain of order  $O(\alpha^2)$ . When perturbation theory is used in this review, we use the expansion in terms of  $\tilde{\alpha} = \tilde{g}^2/(4\pi)$  and try to indicate the expected size of the  $O(\tilde{\alpha}^2)$  terms.

<sup>6</sup> We would like to thank M. Lüscher and S. Sint for pointing out this problem.

left hand side originate from short distances  $|x - y|$  and  $|x - z|$ . At distances of a few lattice spacings, lattice correlation functions do exhibit a strong dependence on the lattice spacing. This will translate into potentially large lattice artifacts of the renormalization constants. A sufficiently small lattice spacing is therefore required to be sure that the  $O(a)$ -terms injected through eq. (2.27) are numerically small. At current values of the lattice spacings, it is not evident that this requirement is fulfilled.

One can avoid this problem at the price of giving up one prediction: In ratios of decay constants, the renormalization cancels and only unavoidable  $O(a)$  terms remain. Unfortunately, this option increases the statistical errors in the decay constants  $f_D$  and  $f_B$  and consequently the remaining  $O(a)$  terms are more difficult to control.

We point out that eq. (2.22) is only an ansatz. In order to systematically reduce the  $O(am_f)$  corrections one has to both improve the action through  $c_{SW} \neq 0$  and the operators. With  $c_{SW} = 1$ , one can achieve  $O(am_f) \rightarrow O(\alpha am_f)$ [40, 29].

In summary, the renormalization of the axial vector current is a nontrivial problem in practice and introduces an uncertainty in the determination of pseudo scalar decay constants. The same holds true for the normalization of four fermion operators such as the one responsible for  $B\bar{B}$  mixing. Furthermore, when working in the HQET in order to evaluate the limiting behavior of the decay constant as one of the quark masses becomes very large, the current develops an anomalous dimension and – at present – no practicable nonperturbative method to renormalize the current is known.

## 2.5 Reaching Asymptotics

In a Monte Carlo simulation one evaluates correlation functions such as eq. (2.13) at finite values of the euclidean time  $x_0$ . In order to be able to extract hadron masses and decay constants, one needs to insure that the terms with  $n > 1$  are negligible in the spectral representation eq. (2.13). For a quantitative investigation of this problem, we consider an example that is relevant for the physics discussed in this review, namely the correlation function of a heavy–light (HL) axial vector current, composed of one heavy quark (with a mass of the order of the charm quark mass) and one light quark.

It is useful to look at the logarithmic slope of the correlation function. This slope, called “effective mass”, approaches a constant when the above mentioned corrections are negligible. In fig. 1 (filled symbols), one observes that the effective mass shows a slow variation with the euclidean time still at a distance of  $x_0 = 15a \sim 5\text{GeV}^{-1}$ . At larger  $x_0$ , a plateau seems to develop in the effective mass. The region of the plateau in fig. 1 is rather short, however.

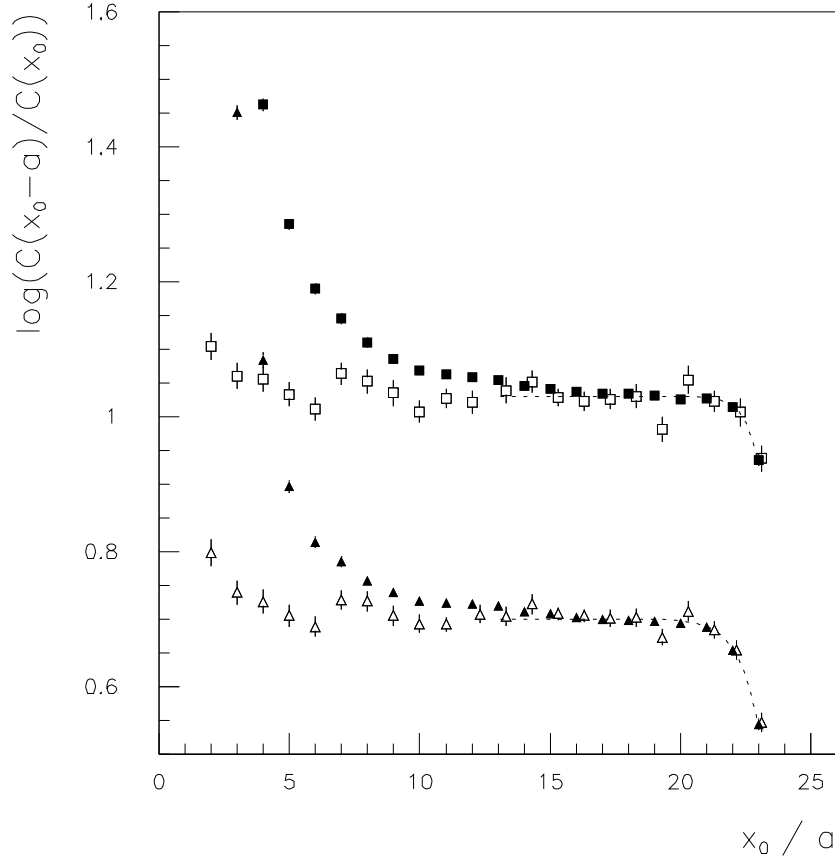


Figure 1: The logarithmic slope of the pseudoscalar correlation functions  $C^{loc,loc}(x_0)$  (filled symbols) and  $C^{G,G}(x_0)$  (open symbols)[44].  $G$  denotes a gaussian wave function with r.m.s. radius of about 0.3 fm. The cutoff is  $a^{-1} = 3.17\text{GeV}$  ( $\beta = 6.26$ ) and the simulation was done in the quenched approximation. The light quark mass was chosen about twice the strange quark mass ( $K=0.1492$ ), while the heavy quark mass is roughly the charm mass ( $K=0.1350$ ) in the lower part and somewhat higher in the upper part ( $K=0.12$ ). The dashed curves illustrate the effect of the finite time extent of the lattice according to eq. (2.31), assuming that only one state contributes in this range of  $x_0$ .



One may improve the situation by choosing better interpolating fields for the hadrons. We briefly describe the approach that has been taken so far for the case of meson fields. The general idea is to “smear” the local quark fields with trial wave functions  $\Phi^J$ :

$$q^J(x) = \sum_y \Phi^J(\vec{x}, \vec{y}; U(y_0)) \delta_{x_0 y_0} q(y) \quad . \quad (2.28)$$

An interpolating field for a meson is then given by

$$\mathcal{M}^J(x) = \bar{q}(x) \gamma_0 \gamma_5 q^J(x) \quad , \quad (2.29)$$

where the index  $J$  denotes the trial wave function and we have omitted the flavor indices<sup>7</sup>.  $\Phi^J(\vec{x}, \vec{y}; U(y_0))$  depends either in a gauge covariant way[41, 42, 43, 46] on the link variables denoted by  $U(y_0)$ , or the construction is done in Coulomb gauge[47]. A meson correlation function is constructed by

$$C^{I,J}(x_0) = \sum_{\vec{x}} \langle \mathcal{M}^I(x) [\mathcal{M}^J(0)]^\dagger \rangle \quad . \quad (2.30)$$

It has the spectral representation

$$C^{I,J}(x_0) = \sum_{n \geq 1} \langle 0 | \mathcal{M}^I(0) | P, n \rangle \langle P, n | [\mathcal{M}^J(0)]^\dagger | 0 \rangle \{ \exp[-E_n x_0] + \exp[E_n(x_0 - L_t)] \} \quad . \quad (2.31)$$

In fig. 1 we have included the logarithmic slope for such a smeared correlation function[44]. It reaches a plateau at values of  $x_0 \sim 5a$  – much earlier than the correlation function of the local axial vector current.

**A clean test for ground state dominance** is provided by the ratio

$$R^{I,J}(x_0) = \frac{C^{I,I}(x_0) C^{J,J}(x_0)}{[C^{I,J}(x_0)]^2} \quad , \quad (2.32)$$

which is constructed such that it becomes one when all correlation functions are dominated by the ground state[44, 45]. This is a very stringent test since contrary to the search for a plateau in the local mass, the value of the plateau is known here too.

Since most computations of  $f_D$  have been carried out implementing the local axial vector current, it is of interest to use this ratio to further investigate in how far the correlation function is dominated by the ground state at accessible values of  $x_0$ . So we display  $R^{G,loc}(x_0)$  in fig. 2 where  $G$  refers to the gaussian smearing already used in fig. 1 and  $loc$  denotes the local axial vector current.  $R^{G,loc}(x_0)$  is only consistent with one for the largest values of  $x_0$ . Therefore, we consider the region of  $x_0$ , where

---

<sup>7</sup> $\Phi$  is the wave function in terms of the relative coordinate. In addition to the form eq. (2.29), the case where both quark fields are smeared has been considered.

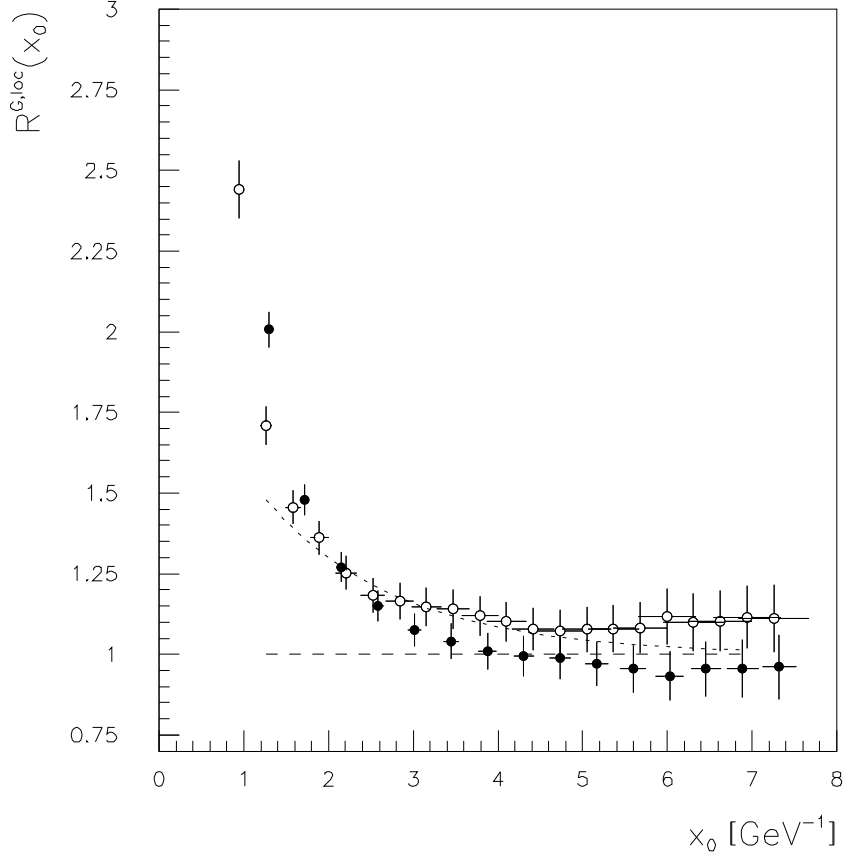


Figure 2: The ratio  $R^{G,loc}(x_0)$  is shown for a light quark mass of about twice the strange quark mass and a heavy quark mass of roughly the charm mass. Open circles are for a cutoff of  $a^{-1} = 3.17\text{GeV}$  ( $\beta = 6.26$ ) and full points are for  $a^{-1} = 2.32\text{GeV}$  ( $\beta = 6.00$ ). The lattice spacing and thus the scale on  $x_0$  are defined through eq. (2.18).

all correlation functions are dominated by the lowest *two* states. There,  $R^{I,J}(x_0)$  is described by

$$R^{I,J}(x_0) = \frac{[1 + \epsilon_I^2 \exp(-x_0\Delta)][1 + \epsilon_J^2 \exp(-x_0\Delta)]}{1 + \epsilon_I\epsilon_J \exp(-x_0\Delta)}, \quad (2.33)$$

$$\epsilon_I = \langle 0|\mathcal{M}^I(0)|P, 2 \rangle / \langle 0|\mathcal{M}^I(0)|P, 1 \rangle, \quad \Delta = E_2 - E_1.$$

Fig. 1 suggests that the smearing wave function was chosen well resulting in  $\epsilon_G \ll \epsilon_{loc}$ . We may therefore simplify further:  $R^{G,loc}(x_0) \sim [1 + \epsilon_{loc}^2 \exp(-x_0\Delta)]$ . A fit to this form is shown as dashed curve in fig. 2. It describes the ratio well with a gap  $\Delta \sim 600\text{MeV}$ . We have thus roughly quantified the dominant correction to the asymptotic behavior of the local axial vector correlation function. The size of this correction term shows us that some of the earlier lattice computations that investigated the dependence of the decay constant of HL mesons on the mass of the meson are subject to a significant

systematic error since they used only local meson fields. One should not regard this investigation as a quantitative determination of the gap in this channel.

If one uses  $C^{loc,loc}$  and does not isolate the ground state properly, one obtains an overestimate of the decay constant. Repeating the above analysis at different values of the heavy quark mass shows that  $\epsilon_{loc}^2$  increases when the heavy quark mass increases, while  $\Delta$  stays roughly constant[44]. Therefore, the effect becomes stronger with increasing quark mass, resulting in a misleading quark–mass dependence. Physically, this effect means that the ratio of the leptonic decay constant of the excited state to the ground state decay constant increases with the mass of the heavy quark. Unfortunately, at present, the precision is not high enough to determine  $\epsilon_{loc}^2$  and its mass dependence well.

A further comment is in order concerning fig. 2: the figure contains results for two values of the cutoff. The ratio has a continuum limit only in the region of  $x_0$  where it is approximated well by the truncated form  $R^{G,loc}(x_0) \sim [1 + \epsilon_{loc}^2 \exp(-x_0\Delta)]$  that was used in the fit. At smaller  $x_0$  where this is not true, nonuniversal matrix elements of the trial wave functions appear and there is no reason to expect an (approximate) independence of the lattice spacing. Therefore, the  $a$ –independence of the ratio that is observed for  $x_0 > 1.5\text{GeV}^{-1}$  is consistent with  $\epsilon_G \ll \epsilon_{loc}$ , that means a well chosen trial wave function in refs. [43, 44].

As a consequence of this investigation, it appears mandatory to use smeared meson fields in order to reach asymptotics and to perform a reliable computation of the decay constant<sup>8</sup>. In order to extract  $f_P$ , the matrix element  $\langle 0|\mathcal{M}^I(0)|P,1\rangle$  which is introduced through the trial wave function, must be cancelled. As seen from eq. (2.31) this can be achieved by combining the results of an analysis of both  $C^{I,I}(x_0)$  and  $C^{I,loc}(x_0)$ .

## 2.6 The Quenched Approximation

As we mentioned in section (2.1), the first step in a Monte Carlo evaluation of the expectation values eq. (2.1) consists of generating lattice gauge fields  $U$  with probability  $\exp(-S_G[U]) \det \mathcal{D}[U]$ . The only algorithm which generates this distribution exactly<sup>9</sup> is the Hybrid Monte Carlo algorithm (HMC). It is numerically quite slow. In particular, the required CPU time for a given simulation scales<sup>10</sup> approximately like  $(m_q a)^{-\eta}$  with  $\eta \sim 5$  [50]. At present, this allows for exploratory simulations at

<sup>8</sup> Of course, the problem can also be solved by going to sufficiently large values of  $x_0$  on a large lattice with large statistics in the Monte Carlo[48].

<sup>9</sup>Actually, the HMC algorithm[49] is valid for pairwise mass degenerate quarks only.

<sup>10</sup> This scaling law includes the scaling of the box length  $L$  that is necessary to avoid finite size effects when going to small quark masses.

unphysically heavy masses  $m_q$  of the quarks.

In perturbation theory,  $\det \mathcal{D}[U]$  generates quark loops. One may assume as a starting point, that for the full path integral at a given value of the cutoff, the effect of the quark loops is mainly to modify the renormalization of the coupling. Therefore, low energy observables may be approximately represented by a model with  $\det \mathcal{D}[U] \rightarrow \text{const.}$  Also the success of constituent quark models suggests that neglecting quark loops in this way may be a sensible approximation to QCD. Clearly, we do expect significant differences between QCD and its quenched approximation, in quantities like flavor singlet densities in hadrons or the connection between the high energy running coupling and hadron masses. In this sense, it is better to think of the “quenched approximation” as a model. It does not constitute a systematic approximation to QCD and its accuracy depends strongly on the quantity that one considers.

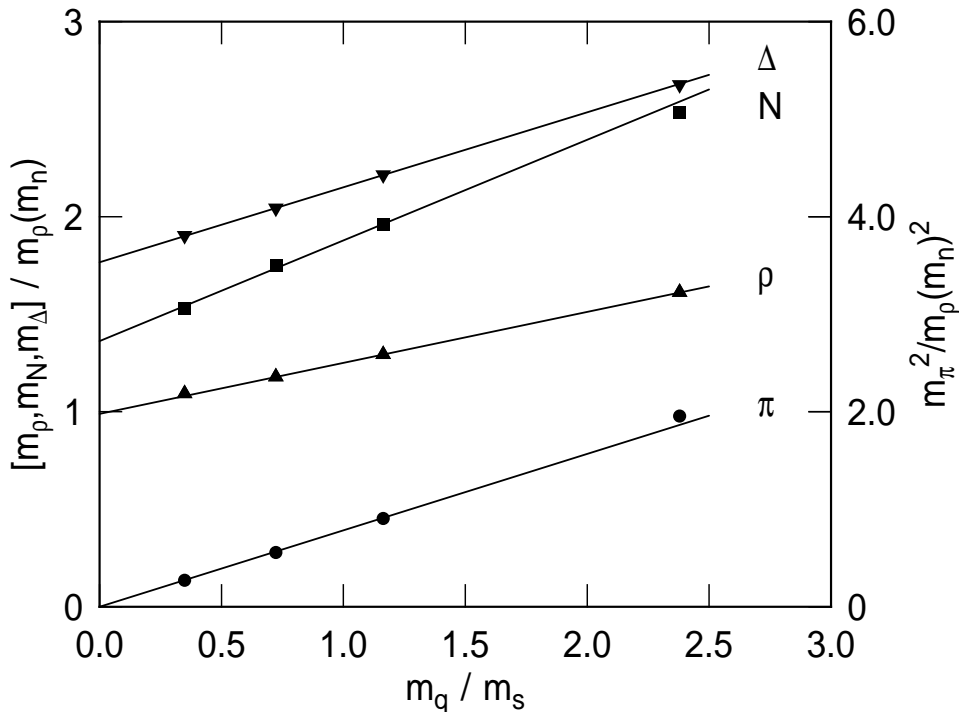


Figure 3: Extrapolation of hadron masses to the chiral limit. The extrapolation curves are used to locate the physical point in the quark mass, that means one point on the renormalization group trajectory. The ordinate  $m_q/m_s$  is the bare quark mass in units of the strange quark mass.  $m_\rho(m_n)$  denotes the  $\rho$ -meson mass at the physical point. The figure is taken from ref. [54]; error bars are smaller than the size of the symbols.

Having emphasized this, we proceed nevertheless to summarize numerical evidence that the “quenched approximation” is surprisingly close to the real world. We consider the low lying hadron mass spectrum. The large effort that went into computing the hadron mass spectrum has been reviewed in references [51, 52]. A significant step on the way towards a reliable computation of the hadron mass spectrum has been taken

by the APE-group, using nonlocal trial wave functions (cf. section 2.5) and quark masses around the strange quark mass[53].

This has recently been improved further in the GF11-project[54] reaching a rather high statistical precision. The latter allowed for a more systematic study of the lattice spacing dependence and the finite volume effects. Using the assumption that up and down quark masses are degenerate, and the quenched approximation, the problem has two parameters only:  $K = K_u = K_d$  and  $g_0^2$ . To get to the physical masses in the continuum limit, one proceeds as discussed in section 2.3. An important difference to the idealization in section 2.3 is that one cannot compute the quark propagators at the physical values of  $K$  since this corresponds to the solution of an almost singular system of linear equations. Instead, all hadron masses are calculated at various values of the hopping parameter  $K$  and then extrapolated using forms suggested by chiral symmetry (for the pion mass) and simple mass perturbation theory. As an illustration, we show the extrapolations that were done in ref. [54] in fig. 3<sup>11</sup>.

In ref. [54] the value of  $K$  at each  $g_0^2$  was fixed requiring  $M_V(K, g_0^2)/M_P(K, g_0^2) = m_\rho/m_\pi$ , where  $M_V$  is the vector meson mass in lattice units and  $m_\rho$  the experimental  $\rho$ -meson mass (the  $\rho$ -meson is a stable particle in the quenched approximation).

The crucial point is now to calculate hadron mass ratios on the renormalization group trajectory and investigate their dependence on the lattice spacing measured as  $M_\rho \equiv m_\rho a$ . Fig. 4 shows the example of  $\frac{M_N}{M_\rho}(M_\rho)$ . A linear dependence on  $M_\rho$  (see section 2.3) is in agreement with the data and gives a value in the continuum limit that is consistent with the experimental value of the mass ratio. The same holds true for  $m_\Delta/m_\rho$ .

In order to compute the masses of strange hadrons as well, Butler et al. assumed first order  $SU(3)_{\text{flavor}}$  symmetry breaking. These results, once they are extrapolated to the continuum, are in agreement with the experiments as well.

In all these cases, the error bars are somewhat large and the number of points is too small to check whether the mass ratios really depend linearly on the lattice spacing. Nonlinear terms could be important in this range of lattice spacings. To some extent, we can investigate this question by using another precision-quantity: the potential  $V(r)$  between static quarks can be calculated very precisely in lattice QCD. A well calculable length scale  $r_0$  may be obtained from the force  $F(r) = \frac{d}{dr}V(r)$  through the implicit definition  $F(r_0)r_0^2 = 1.65$ [30]. The constant 1.65 is chosen such that one

---

<sup>11</sup> There are strong arguments[55] that the quark-mass dependence of hadron masses is more complicated in the quenched approximation. It may be non-analytic at zero quark mass. It is, however, not obvious at which values of the quark mass such behavior sets in. Furthermore, such non-analyticities would mean that observables that are calculated in the quenched approximation deviate very significantly from the true result when the quark masses approach zero. Therefore, one should stay away sufficiently far from the chiral point and extrapolate using the mass dependencies expected for full QCD.

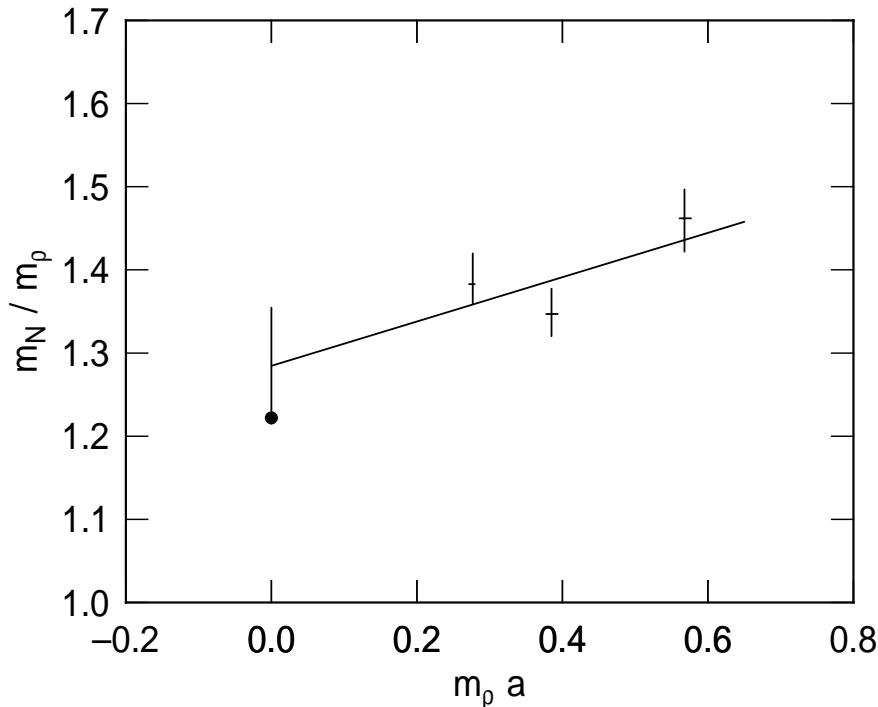


Figure 4: Extrapolation of the nucleon to  $\rho$  mass ratio to the continuum limit. The figure is taken from ref. [54].

obtains  $r_0 \sim 0.5$  fm when one uses the force derived from potential models that successfully describe the  $b\bar{b}$  spectra (0.5 fm is about the distance, where the phenomenological potential models are most severely restricted by the spectrum).  $r_0$  has not been determined at all values of the bare coupling which we need here. We therefore take the following approach: at distances  $r\sqrt{\sigma} > 0.3$  the potential is well described by

$$V(r) = \pi/(12r) + \sigma r \quad , \quad (2.34)$$

with  $\sigma$  representing the string tension<sup>12</sup>. We use  $\sigma$  as defined in eq. (2.34), noting that through the very parametrization of the potential one has  $\sqrt{\sigma}r_0 \equiv 1.18$ . For the precision that is required in the following, the uncertainty due to the parametrization eq. (2.34) is irrelevant. In the future, when hadronic masses with higher precision are available, it will be important to use the direct definition of  $r_0$ .

We have combined the data obtained from the simulations of ref. [58, 57] as listed in [43] with masses of the  $\rho$ -meson from ref. [54, 53, 44, 59]<sup>13</sup> to form the ratio  $M_\rho/\sqrt{\Sigma}$ . (By  $\Sigma$  we denote the estimate of  $\sigma$  at a finite value of  $a$  in lattice units:  $\Sigma = a_\sigma^2\sigma$ .)

<sup>12</sup> The subleading term  $\pi/(12r)$  is the universal first correction of an effective bosonic string[56]. It is both in agreement with SU(3) gauge theory simulations and with the force in the continuum limit of the SU(2)-theory[30].

<sup>13</sup> In three cases (for  $L/aM_\rho < 6$ ) it was necessary to correct the mass of the  $\rho$ -meson for a

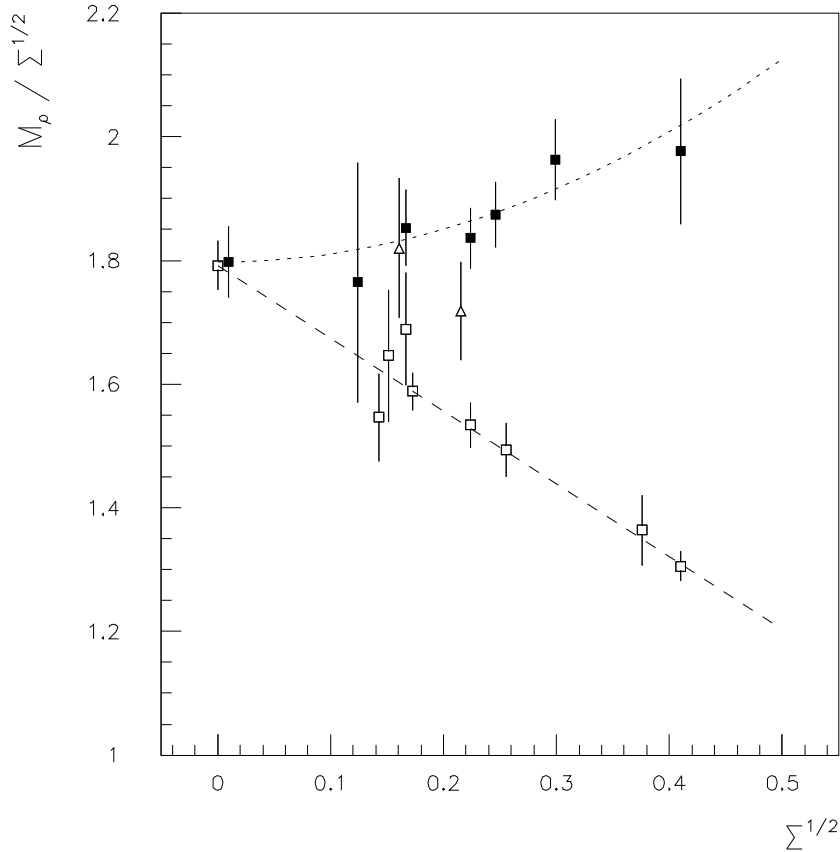


Figure 5: The lattice spacing dependence of  $M_\rho/\sqrt{\Sigma}$  for three different fermionic actions: Wilson action (full squares [54, 53, 44, 59]), Sheikholeslami Wohlert action (triangles [59, 66, 67]) and staggered fermion action [90] (filled squares [61, 62, 63, 64]).

The lattice spacing dependence of  $M_\rho/\sqrt{\Sigma}$  is shown in fig. 5 (open squares). A linear relation describes the data well in the whole range. The range of lattice spacings that is covered here includes the one in the extrapolations of [54] but it extends further towards  $a = 0$ . The linearity observed in fig. 5 lends support to the extrapolations [54] that we discussed above.

The extrapolation of  $M_\rho/\sqrt{\Sigma}$  is further checked by computations that were done using different forms of the fermion action. 1) The  $\rho$ -mass data of various groups [61, 62, 63, 64] using the staggered fermion action [90] (filled squares) have corrections to the continuum limit of the opposite sign. For this fermion action, mass ratios should approach their continuum limit with corrections proportional to  $a^2$  [65]. This form

---

slight finite volume effect [60]. The correction was taken from [60] and its uncertainty was taken into account.

is fitted to the data. As a result we observe **universality** in the continuum limit despite the quite significant differences at finite values of the lattice spacing! The figure underscores the importance of performing such extrapolations in order to obtain the physical continuum limit numbers. 2) The recent computations by the UKQCD-group[59] and the APE-group[66, 67], using the improved action are represented by the triangles. Although the error bars are somewhat large to draw definite conclusions, it appears to be close to the above continuum limit extrapolations indicating small discretization errors. Further points for larger values of the lattice spacing in this plot could clearly settle the question to which extent the improved action of Sheikholeslami and Wohlert reduces the  $O(a)$  scaling violations in nonperturbative quantities.

Altogether the investigation of the lattice spacing dependence and universality of  $M_\rho/\sqrt{\Sigma}$  provides further support for the continuum limit extrapolations of mass ratios of Butler et al. As the extrapolated numbers agree with the experimental observations to within  $\sim 10\%$ , one may conclude that the quenched approximation is at least a good *model* for QCD. In fact, it appears to be the best model of QCD that we have, considering that it contains only the fundamental parameters of QCD as unknowns. However, we would like to emphasize again that there is an unknown systematic error involved when we replace QCD by this model for calculating a new quantity.

We do not want to review the numerous efforts that have been made to directly compare QCD and its quenched approximation (at a given value of the cutoff). Instead, we refer the interested reader to review articles on this subject[51, 52]. Sea quark masses of around the strange quark mass and higher have been used so far. For these quark masses, no significant changes in the physical observables have been found apart from the aforementioned change in the coupling constant at the cutoff scale. This is in agreement with the conclusion drawn in the previous paragraph.

## 2.7 The $b$ -Quark on the Lattice

In the previous sections, we have discussed the general problems in practical lattice QCD calculations. Apart from renormalization of operators, the dependence of lattice results on the spacing  $a$  is most important. As long as we are considering hadrons consisting of light quarks such as  $u, d$  and  $s$ , it is sufficient to have a good resolution of the wave-function in order for  $a$ -effects to be moderate and to be able to extrapolate to the continuum limit.

When one considers bound states of a heavy quark like the  $b$ -quark with other constituents, it is necessary to have

$$m_h a \ll 1 \tag{2.35}$$

in addition. (We denote a generic heavy quark by  $h$ .) In a given background gauge



field, the heavy quark only propagates correctly under this condition.

This condition is hard to fulfill for the following reason. In order to control finite size effects in hadron masses and matrix elements, we need to compute with a box size of the order of more than one fermi (see section 3.2). Even a lattice with  $L/a = 32$  points has  $m_b a > 1$  for these values of  $L$ . Consequently, a direct simulation of the  $b$ -quark requires finer lattices than the ones that have been technologically accessible so far. One had to search for alternatives to a simulation with fully propagating  $b$ -quarks.

Intuitively, one expects that (for low energy matrix elements) the high frequency parts of the propagation of a heavy quark can be absorbed into local terms of an effective action[68]. It should therefore be possible to work with a modified action and a cutoff  $a^{-1} \ll m_b$  as long as one is only interested in long distance observables.

Through a formal expansion in  $1/m_h$  one obtains the non-relativistic QCD action[68]

$$S_{NRQCD} = \phi^\dagger \left[ D_0 - \frac{\vec{D}^2}{2m_h} - \frac{\vec{\sigma} \vec{B}}{2m_h} \right] \phi + O(1/m_h^2), \quad (2.36)$$

written here in terms of the covariant derivative  $D_\mu = (D_0, \vec{D})$  [23] and the chromo magnetic field strength,  $\vec{B}$ . In this formulation, the heavy quark field  $\phi$  is a 2-component spinor field and  $\vec{\sigma}$  is a vector composed of the three Pauli matrices.

Beyond the formal level, the use of the effective action eq. (2.36) is nontrivial. The theory defined through  $S_{NRQCD}$  and its appropriate regularization is nonrenormalizable. A finite cutoff has to be kept. The condition  $a^{-1} \ll m_b$  requires that computations have to be done just in the opposite range from eq. (2.35). This means the lattice spacing is in the middle of the range in fig. 5. For such resolutions, one has to worry about the effects of order  $O(a)$  as it is clearly demonstrated in that figure. These cannot be removed by extrapolation  $a \rightarrow 0$  since that limit does not exist. Instead,  $O(a)$ -effects have to be reduced by adding new (higher dimensional) operators to the action. Their coefficients need to be determined by matching a number of observables in the effective theory to the observables in the full theory. One possibility is to match directly to experimental observations. This procedure both reduces the predictability of the theory and introduces statistical errors into the coefficients. The second possibility is to estimate the coefficients through mean field theory or by matching perturbatively[69].

Concerning the second choice, it is likely that incalculable nonperturbative contributions in the coefficients induce finite terms into the final physical matrix elements that are of the same order as the physical result that one wants to calculate[70]. This possibility originates from the powerlaw divergencies of the effective theory[70]. It is argued, however, that such terms should be small numerically[71, 33].

According to our judgment, it will be difficult to quantify the uncertainty due to either missing higher order terms in the action or the incalculable nonperturbative contributions to the coefficients of the effective action. Currently, non-relativistic QCD on the lattice is under intense investigation[72].

It is important to notice, that these problems of non-relativistic QCD do not exist when one truncates the action eq. (2.36) after the first term[73, 74]. It has been suggested by Eichten[75] to apply this  $O((1/m_h)^0)$  approximation to the b-quark on the lattice. This treatment of a heavy quark is called the **static approximation**, since the heavy quark is represented by a static color source [75, 76]. Its propagator  $S_h(x, y)$  in a given background field is just a Wilson line:

$$S_h(x, y) = \delta_{\vec{x}, \vec{y}} (1 + \gamma_0)/2 W^\dagger(x_0, y_0; \vec{x}) \quad \text{for } x_0 > y_0 \quad ; \quad (2.37)$$

$$W(x_0, y_0; \vec{x}) = \prod_{z_0=x_0}^{y_0-a} U_0(z = (z_0, x_1, x_2, x_3)) .$$

In the static approximation, the only powerlaw divergent – and therefore incalculable in perturbation theory – renormalization is the renormalization of the quark mass. The latter is of limited physical interest. Most importantly, the renormalization of the axial vector current can be calculated in perturbation theory[73, 74] allowing for a computation of the decay constant in this approximation.

One can therefore compute properties of B-mesons through the following strategy. As a first step, one determines their limiting behavior for  $m_h \rightarrow \infty$  using the static approximation. Then one investigates their dependence on the mass of the heavy quark for masses as large as possible and finally one interpolates between the results at finite values of the meson mass and in the static approximation. The interpolation is done in the form suggested by the  $1/m_h$ -expansion, but the coefficients of the different powers of  $1/m_h$  are not computed explicitly since they suffer from powerlaw divergencies[70]. Rather they are taken from the phenomenological matching between finite mass and infinite mass results.

### 3. The Leptonic Decay Constants $f_D, f_{D_s}$

This section is a review of the computations of heavy light decay constants for heavy quark masses around the mass of the  $c$ -quark. As a general orientation, we list in table 1 the results that have been quoted in the literature. Note that the different computations have used different renormalization constants and different ways to determine the lattice spacing. At finite values of the lattice spacing and in the quenched approximation this can introduce quite significant variations. This explains the spread of the values given in table 1.

Ref.	$f_D$ [MeV]	$f_{D_s}/f_D$	$a_\sigma^{-1}$ [GeV]	$n_f$
[78]	$174 \pm 26 \pm 46$	$(f_{D_s} = 234 \pm 46 \pm 55 \text{ MeV})$	2.2	0
[79]	$197 \pm 14$		1.9	0
[79]	$181 \pm 27$		2.6	0
[80]	$190 \pm 45$	$1.17 \pm 0.22$	1.9	0
[19]	$198 \pm 17$	$(f_{D_s} = 209 \pm 18 \text{ MeV})$	1.9	0
[81]	$210 \pm 15$	$1.08 \pm 0.02$	1.9-3.4	0
[82]	$208 \pm 9 \pm 35 \pm 12$	$1.11 \pm 0.05$	2.9	0
[46]	$185_{-3}^{+4} \text{ }_{-7}^{+42}$	$1.18 \pm 0.02$	1.9-2.6	0
[44]	$170 \pm 30$	$1.09 \pm 0.02 \pm 0.05$	1.1 - 2.8	
[83]	$283 \pm 28$		$\sim 1.5$	2
[77]	130 - 300	$(f_{D_s} = 170 - 395 \text{ MeV})$	$\sim 1.5$	2

Table 1: A compilation of published values of the decay constants in the D-system. Note that the treatment of systematic errors is very different in the different works( In particular, the large range quoted in [77] is due to a conservative estimate of the systematic errors, while [83] did not estimate systematic errors.) All computations use the Wilson action ( $c_{SW} = 0$ ) except for ref. [46], which uses the treelevel  $O(a)$  improved action( $c_{SW} = 1$ )[24]. The fourth column gives the value of the cutoff estimated from the string tension as  $a_\sigma^{-1}[\text{GeV}] = 0.420 / \sqrt{\Sigma}$ .

In order to combine the information from the different publications, it is necessary to separately investigate each of the possible sources of systematic errors. A good statistical accuracy is needed before systematic errors can be investigated in a meaningful way. The pioneering computations[78, 79, 80, 19] did not have a sufficient accuracy for that purpose. Therefore, we will only use the results of refs. [82, 46, 44, 77, 67] in the following. It also would have been of great use to include the computation that was performed at the smallest value of the lattice spacing[81]. Unfortunately, applying what we learned in section 2.5 about the effects of excited states to that computation shows that systematic errors due to excited states are of the order of the statistical errors. Consequently it is not included in the following. The same holds true for part of the results of ref. [84]; the conclusions of that paper have to be revised. The data that we do include in the following discussion[82, 46, 44, 77] either was obtained by appropriate smearing techniques or at sufficiently large separations  $x_0$ . Uncertainties

due to excited state contributions should be well below the statistical errors.

### 3.1 Extrapolation to Light Quark Masses

In the work mentioned above, all extrapolations are performed as follows. Motivated by chiral perturbation theory[85] one fits

$$M_P^2(g_0^2, K_f, K_{f'}) = A(g_0^2) \left( \frac{1}{2K_f} + \frac{1}{2K_{f'}} - \frac{1}{K_{crit}} \right) \quad (3.1)$$

to determine  $A(g_0^2)$  and  $K_{crit}$ . Then the points on the renormalization group trajectory corresponding to the s- quark and the u/d-quark may be fixed by requiring the pion and the Kaon to acquire their physical mass in units of the string tension or another dimensionful observable such as  $f_\pi$

$$A(g_0^2) \left( \frac{1}{K_u} - \frac{1}{K_{crit}} \right) / \Sigma = m_\pi^2 / \sigma \quad (3.2)$$

$$A(g_0^2) \left( \frac{1}{2K_u} + \frac{1}{2K_s} - \frac{1}{K_{crit}} \right) / \Sigma = m_K^2 / \sigma \quad (3.3)$$

with  $m_\pi = 137$  MeV,  $m_K = 490$  MeV and  $\sigma \sim 420$  MeV.

Other quantities, such as masses and decay constants of HL-mesons, have a much weaker dependence on the bare quark mass. They are extrapolated linearly in  $1/K_f$  to the corresponding points  $K_f = K_u$  or  $K_f = K_s$ . The linear behavior is confirmed in all simulations (within the errors). So, for the quantities discussed here, the extrapolations appear to be quite reliable and are not discussed any further<sup>14</sup>.

We proceed now to investigate finite size effects, the lattice spacing dependence and renormalization in the quenched approximation to arrive at an estimate of the decay constant in that model. In a final subsection, we will try to see to what extent light sea quarks alter that result.

### 3.2 Finite Size Effects

At asymptotically large lengths  $L$  of the box, the dominant finite size effects originate from a self interaction of the meson through an exchange of a particle with the quantum numbers of the vacuum. The particle can propagate once around the world, introducing an  $L$ -dependence. In the quenched approximation the relevant lightest

---

<sup>14</sup> We note that the choice of scale (namely  $\sigma$  in the above equations) influences the precise values of  $K_u$  and  $K_s$ . Numerically, it is not important in the following, however.

particle is the  $0^{++}$  glueball. The effect is suppressed exponentially in  $L$  with a decay rate of the inverse glueball mass. For lattice sizes that are being used in the simulations of HL-mesons the product  $Lm_{0^{++}}$  is larger than ten[86, 87]. This mechanism for finite size effects is therefore irrelevant in the present context.

The dominant finite size effects within an intermediate regime should originate from a distortion of the wave function in the finite volume. In a nonrelativistic potential model, the rms-radius of an HL-meson is significantly smaller than the rms-radius of a LL-meson since the reduced mass is smaller by almost a factor of two. Taking a look at LL-meson decay constants that are published in the literature, a size-dependence is not visible for  $L\sqrt{\Sigma} \sim 3$  and larger. As a result, we clearly do not expect relevant finite size effects for HL-mesons once  $L$  is in that range.

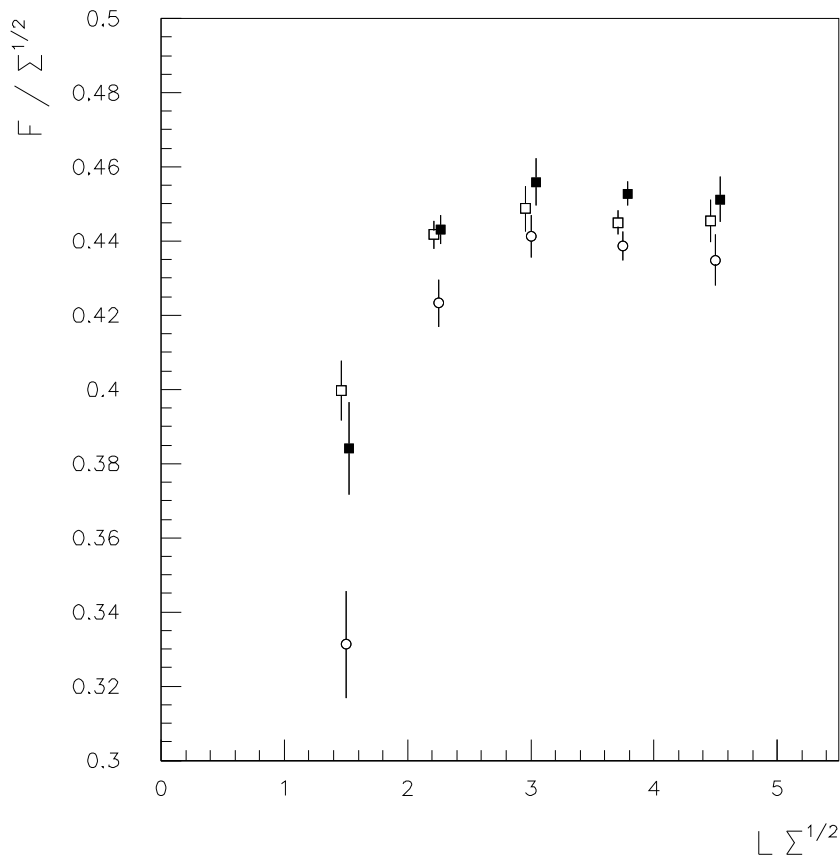


Figure 6: The dependence of the HL pseudo scalar decay constant  $F$  on the box size  $L$ [44]. The light-quark mass is fixed at about twice the strange quark mass and the meson mass varies from about 0.8 GeV (circles) to 1.5 GeV (filled boxes).

Indeed, as shown in fig. 6, numerical investigations with moderate light-quark masses and varying mass of the heavy quark, confirm the expectation[44].

One may speculate further that the finite size effects seen within the regime of  $L\sqrt{\Sigma} \sim 1.5 - 2$  originate from a distortion of the light-quark wave function in the finite volume. For an exponentially decaying wave function, the finite size effects on the wave function at the origin are again exponential in  $L$ . The characteristic scale is the coefficient in the falloff of the wave function. A rough estimate of 1.5 in units of the string tension is derived from the Bethe–Salpeter wave function of HL and static-light mesons in Landau gauge[88]. The data in fig. 6 suggests an even larger coefficient of the falloff if one fits to an exponential law in the whole range. Consequently, finite size effects are expected to be smaller than the statistical errors when  $L\sqrt{\Sigma} \sim 3$ . They are neglected in the following. This statement is checked by the data on the level of  $\sim 5\%$ [44]. Note that finite size effects must be reevaluated once future investigations reach higher precisions.

### 3.3 Lattice Spacing Dependence and Renormalization

The most important systematic uncertainty of the decay constant originates from the dependence on the lattice spacing. In principle, the cleanest way of investigating this dependence and altogether removing the uncertainty through an extrapolation to the continuum is the following.

One fixes the hopping parameter of the light quark  $K_u$  as described above and the hopping parameter of the charm quark  $K_C$  is determined through

$$M_P(K_C, K_u, g_0^2)/F_P(K_u, K_u, g_0^2) = m_D/f_\pi . \quad (3.4)$$

At these values of the hopping parameters one considers the ratio

$$Q(g_0^2) = F_P(K_C, K_u, g_0^2)/F_P(K_u, K_u, g_0^2) . \quad (3.5)$$

Up to lattice artifacts, this is the ratio of the D–meson decay constant to the pion decay constant  $f_\pi$ :

$$Q(g_0^2) * f_\pi = f_D + O(a) . \quad (3.6)$$

In the literature this is called “setting the scale through  $f_\pi$ ”. The advantage over every other method is that the renormalization of the axial vector current (see section 2.4) cancels, apart from its dependence on the mass in lattice units, which represents a lattice artifact. This means that the axial vector current is renormalized nonperturbatively.

With increased statistical precision, this method should give the most reliable determination of  $f_D$ . At present, the error bars of  $F_P(K_u, K_u, g_0^2)$  are relatively large and dominate the errors of the ratio  $Q$ . Therefore, the  $O(a)$  terms cannot be detected well enough to allow for a continuum extrapolation using eq. (3.6).

Consequently, it is advantageous to follow a detour when one wants to exploit the results presently available. We split  $Q$  into

$$Q(g_0^2) = q_1(g_0^2)/q_2(g_0^2), \quad (3.7)$$

$$q_1(g_0^2) = F_P(K_C, K_u, g_0^2)/\sqrt{\Sigma}, \quad q_2(g_0^2) = F_P(K_u, K_u, g_0^2)/\sqrt{\Sigma}. \quad (3.8)$$

Then  $q_1(g_0^2)$  and  $q_2(g_0^2)$  can be extrapolated separately to the continuum limit and  $f_D$  is calculated by their ratio in the continuum limit.

Since the renormalization of the axial vector current is known to one-loop order only, there are in addition to the terms of order  $O(a)$ , errors of order  $O(\tilde{\alpha}^2)$  in  $q_1$  and  $q_2$ . From the work of Lepage and Mackenzie[35], it appears justified to assume that these missing terms have coefficients of order one. A coefficient of four would mean  $4 \tilde{\alpha}^2 \sim 2\%$  to  $8\%$  in the range of cutoffs that are considered below. As it will become evident below, an uncertainty of that order does not need to be too disquieting. In addition, the same systematic uncertainty is present in  $q_1$  and  $q_2$  and the effect of the uncertainty on the extrapolation will cancel partly when one takes the ratio.

The two advantages of this procedure are that i) the lattice spacing dependence of  $q_1$  can be studied with small statistical errors and ii) additional data at other values of  $g_0^2$  are available for the pion decay constant. Due to this additional data, most notably the one of ref. [89],  $q_2$  can be extrapolated quite well. To do this, we have taken the data for  $f_\pi$  from the literature[82, 89, 44, 53, 59] and applied the perturbative renormalization of the axial vector current eq. (2.24).

We show the extrapolation of  $q_2$  to the continuum in fig. 7. The lattice spacing dependence is very weak and we obtain in the continuum limit of the quenched approximation:  $f_\pi/\sqrt{\sigma} = 0.270(12)$ . The error does not contain the (maybe around 5%) uncertainty due to the missing terms of order  $O(\tilde{\alpha}^2)$  in the perturbative renormalization.

Fig. 7 also contains results obtained with the improved action. Within their uncertainty they coincide with the Wilson-data. This is in agreement with the assumption that both lattice spacing effects and higher order perturbative terms in the renormalization are small.

The extrapolation of  $q_1$  is a more difficult task. Fig. 8 summarizes the available data of sufficient precision. The filled squares are results with the Wilson action, the normalization eq. (2.21) and 1-loop perturbative  $Z_A$ . The open squares are the same data with normalization eq. (2.22). It is more than apparent that the lattice spacing dependence is stronger for this normalization. This matches completely with the case of the local vector current renormalization discussed in the appendix. From a theoretical point of view, one can only speculate about this surprising result. It is helpful to recall that lattice artifacts originate both from the operators in a correlation function





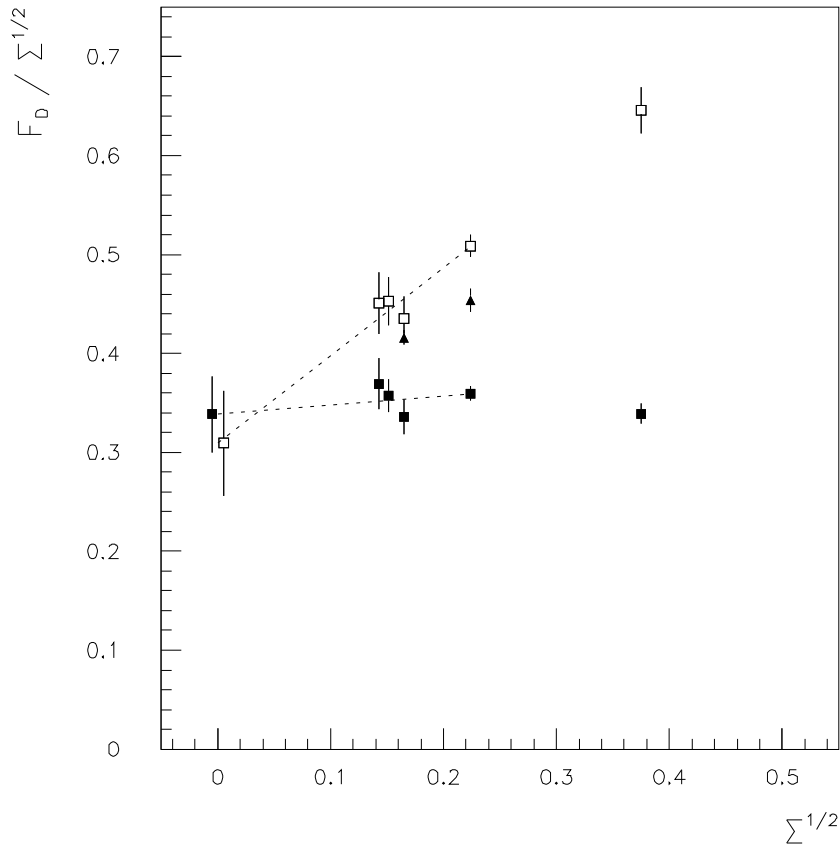


Figure 8: The lattice spacing dependence of the D-meson decay constant. The data with the Wilson action are from ref. [82] (first point) ref. [67] (third point) and ref. [44]. The triangles represent the results with the improved action. They are from ref. [67] (first point) and [46] (second point).

large difference of the different data sets simply reflects that the mass of the charm quark in lattice units is quite large at least for  $\sqrt{\Sigma} > 0.3$ . Therefore, we omit the point with the largest value of the lattice spacing and extrapolate the others linearly in  $\sqrt{\Sigma}$ . The points at  $\Sigma = 0$  in fig. 8 show the results of the extrapolations. They are consistent and furthermore, results within those error bars would be obtained if one included the points at the largest value of the lattice spacing. We take this as evidence that the error bars include the systematic error from the extrapolation. In particular, the full squares extrapolate to  $f_D/\sqrt{\sigma} = 0.338(39)$ . The uncertainties due to the perturbative renormalization are as above.

### 3.4 Estimate in the Quenched Approximation

We combine  $f_D/\sqrt{\sigma} = 0.338(39)$  and  $f_\pi/\sqrt{\sigma} = 0.270(12)$  to attain

$$f_D/f_\pi = 1.25(15) . \quad (3.9)$$

Here, we have neglected the  $O(\tilde{\alpha}^2)$  renormalization error. This uncertainty, which may be sizeable in the individual ratios  $q_i$ , should cancel out to a large degree when one forms  $f_D/f_\pi$ . In particular, we may also regard the fitted function in fig. 7 as a legitimate interpolation of the data. Since it does not have any significant  $a$ -dependence, the ratio  $F_D/\sqrt{\Sigma}$  contains to a reasonable approximation the full  $a$ -dependence of the ratio  $Q$ . As explained above,  $Q$  has only  $O(a)$  effects and no  $O(\tilde{g}^4)$  corrections. Consequently, the linear extrapolation of  $q_1$  and  $q_2$  separately seems justified at the present level of precision.

The above value corresponds to  $f_D = 164(20)$  MeV.

Regrettably, the computations with the improved action do not yet cover a sufficient range of lattice spacings to perform such an analysis. As seen in figs. 7, 8, the data are in agreement with the ones obtained with the Wilson action so far.

### 3.5 Full QCD

Simulations of full QCD have so far mainly been carried out using the staggered fermion action[90]. In this case, one has fewer degrees of freedom, which renders the simulations more tractable. Unfortunately, no results for HL-mesons exist with that discretization of QCD. It appears to be particularly difficult to find operators that have sufficient projection onto the ground state in the HL channel when using this action[91].

In two publications, listed as the last two lines in table 1, decay constants of HL-mesons are computed with the Wilson action. Ref. [83] presents a very exploratory simulation with an approximate algorithm to account for the fermion determinant. On the other hand, ref. [77] simulates with the Hybrid Monte Carlo algorithm with two different sea quark masses, one of which is some 25% below the strange quark mass and the second one is  $\sim 15\%$  above the strange quark mass. The lattice spacing determined from the mass of the  $\rho$ -meson is around  $a = 1/(1.5 \text{ GeV})$ . This corresponds to  $\sqrt{\Sigma} \sim 0.38$ , the point with the largest lattice spacing in fig. 8. Consequently, the systematic errors due to a finite lattice spacing are estimated to be rather large[77], which results in the wide range for  $f_D$ ,  $f_{D_s}$  that is quoted in table 1.

We want to go somewhat beyond the interpretation of the data presented in ref. [77].

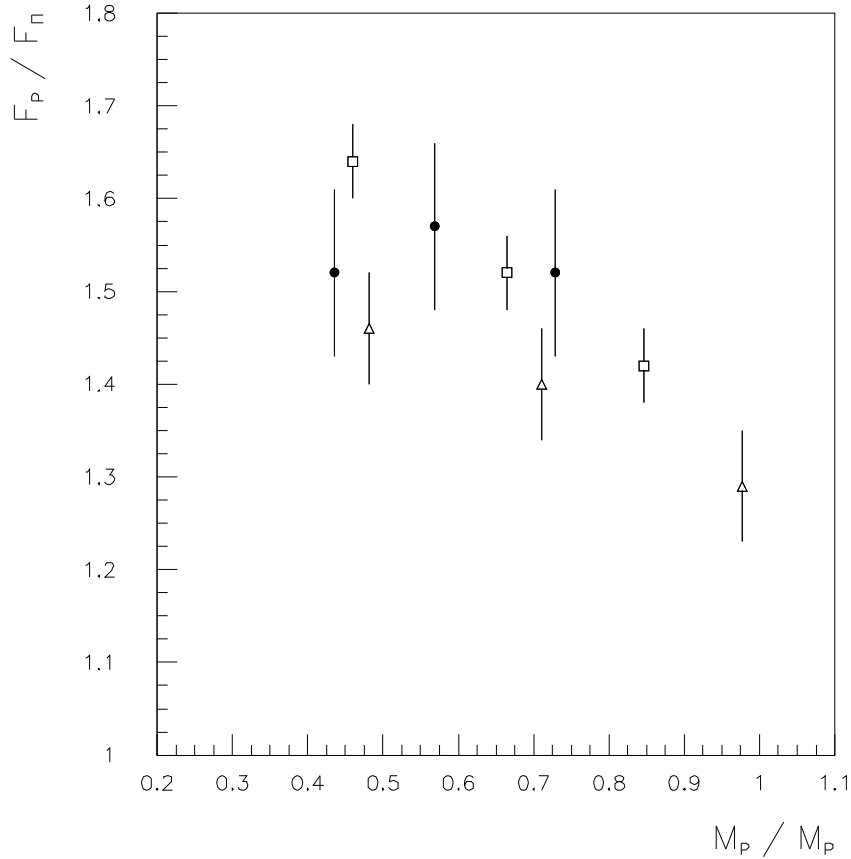


Figure 9: The ratio  $F_P(g_0^2, K_l, K_h)/F_P(g_0^2, K_u, K_u)$  as a function of  $M_V(g_0^2, K_u, K_u)/M_P(g_0^2, K_l, K_h)$ . Open symbols are for  $n_f = 2$  [77] with  $K_l$  somewhat below  $K_s$  (squares) and  $K_l$  somewhat above  $K_s$  (triangles). Filled circles are for  $n_f = 0$  and  $K_l = K_s$  [44].

For the hadron mass spectrum, dynamical fermion simulations have yielded results that are completely compatible with the quenched spectrum *at the same value of the lattice spacing*. It is in fact quite plausible that one should compare at a fixed value of the cutoff, since if one has a small effect of quark loops on a certain observable it is natural that also the lattice artifacts do not feel much of the presence of dynamical fermions.

In order to test to what extent this statement is correct for HL decay constants, we compare the numbers given in the tables in ref. [77] with the quenched data of ref. [44] at  $\sqrt{\Sigma} \sim 0.38$ . The systematic uncertainty on  $Z_A$  is eliminated by looking at the ratio of HL-decay constants to the pion decay constant<sup>15</sup>. A further uncertainty originates

<sup>15</sup> We used the normalization eq. (2.21). Inserting eq. (2.22) would result overall in quite different numbers, but the agreement of the quenched QCD with the full QCD results would be just as good.

from the masses of the quarks. In fig. 9, we show the quenched result for the strange quark mass and the results with  $n_f = 2$  for the two sea quark masses that straddle that mass. The heavy quark mass varies along the  $x$ -axis where the mass of the meson is given in units of  $m_\rho$ .

Remembering that the quenched mesons have a light-quark mass in between the two (independent) simulations with dynamical fermions, there is complete agreement between the two sets of data. We may take this as positive evidence - albeit with a precision of maybe 10% - that there is no effect of dynamical fermions on the decay constants. Of course, this is a check at *one* relatively large value of the lattice spacing and one cannot exclude a somewhat different result at a smaller value of  $a$ . We should remember further that the light quarks have masses around the strange quark mass in this test.

Further tests with smaller  $a$  and smaller quark masses will become possible soon.

## 4. The Leptonic Decay Constants $f_B, f_{B_s}$

Computations of properties of B-mesons are considerably more difficult than the ones discussed in the previous section because of the large mass of the b-quark (cf. section 2.7). At present, appropriate values of the lattice spacing, i.e. such that  $m_b a \ll 1$ , have not been reached.

Therefore, the estimation of  $f_B$  starts from the limiting value obtained in the approximation of neglecting terms of order  $O(m_b^{-1})$ . Next, one investigates the mass dependence of HL decay constants for varying masses of the heavy quark, where those masses are around the mass of the charm quark. Finally, one matches the two results through some interpolation and arrives at an estimate of  $f_B$ . We describe these steps in the following three sections.

### 4.1 Static Approximation

Using a static propagator eq.(2.37) for a B-meson, the (bare) axial vector correlation function does not depend on the mass of the heavy quark. So, the combination  $F_P \sqrt{M_P}$  does not depend on the mass of the quark in the bare regularized theory. Since we are working with an effective action for the heavy quark, we have to restore the relation to QCD by matching the effective theory to QCD [73, 74]. It is most transparent to require directly that the correlation function eq. (2.13) is the same in the effective theory and in QCD up to terms of order  $O(m_h^{-1})$  [73]. To 1-loop order perturbation theory this is achieved after accounting for a (linearly divergent) subtraction of the binding energy and a renormalization of the axial vector current by a factor [73, 74, 92]

$$Z_{\text{stat}}(a m_h) = 1 + \tilde{\alpha} \left[ \frac{1}{\pi} \log(a m_h) - 2.372 \right], \text{ for } c_{SW} = 0, \quad (4.1)$$

$$Z_{\text{stat}}(a m_h) = 1 + \tilde{\alpha} \left[ \frac{1}{\pi} \log(a m_h) - 1.808 \right], \text{ for } c_{SW} = 1. \quad (4.2)$$

In the static approximation one thus computes

$$\hat{F}^{\text{stat}} = Z_{\text{stat}}(a m_b) \langle 0 | \bar{q}_h \gamma_0 \gamma_5 q_l(0) | P \rangle |_{\text{stat}}, \quad (4.3)$$

where, because of the physical interest, we have renormalized at  $m_b$ .  $\hat{F}^{\text{stat}}$  contains the full information on the decay constant that can be obtained in the static approximation in the form [93]

$$\hat{F}^{\text{stat}} = \lim_{M_P \rightarrow \infty} \hat{F}(M_P) \quad (4.4)$$

$$\hat{F}(M_P) = F(M_P) \sqrt{M_P} \left( \frac{\alpha_s(M_P)}{\alpha_s(M_B)} \right)^{2/\beta_0}; \quad \beta_0 = 11 - \frac{2}{3} n_f, \quad (4.5)$$

where  $n_f$  is the number of dynamical quark flavors (Here the leading logarithms have been summed using the renormalization group equation and the difference between the mass of the meson and the mass of the quark has been neglected).

As a first overview of the effort that went into the computation of  $\hat{F}^{\text{stat}}$ , we list in table 2 the different published computations of  $f^{\text{stat}} = a^{-3/2} \hat{F}^{\text{stat}} / \sqrt{m_B}$ . Here, one has to note, that part of the scatter in the table originates from different ways of setting the scale and other systematic errors, which we attempt to analyze below.

Ref.	$f_{B_d}^{\text{stat}} [\text{MeV}]$	$f_{B_s}^{\text{stat}} / f_{B_d}^{\text{stat}}$	$a_\sigma^{-1} [\text{GeV}]$	$c_{SW}$
[94]	$< \sim 260$		1.9	0
[18]	$310 \pm 25 \pm 50$		1.9	0
[19]	$366 \pm 22 \pm 55$	1.10	1.9	0
[43]	$230 \pm 22 \pm 26$	1.16	1.4 - 2.7	0
[66]	$350 \pm 40 \pm 30$	$1.14 \pm 0.04$	1.9	0
[95]	$319 \pm \times \frac{Z}{0.79} \times \left(\frac{a^{-1}}{1.75 \text{GeV}}\right)^{3/2}$		1.6	0
[82]	$235 \pm 20 \pm 21$	$1.11 \pm 0.04$	2.9	0
[66]	$370 \pm 40$		1.9	1
[46]	$253_{-15}^{+16} \quad +105_{-14}$	$1.14_{-0.03}^{+0.04}$	2.6	1

Table 2: A compilation of published values of the decay constants in the B-system as they were obtained in the *static approximation*. The fourth column gives the value of the cutoff estimated from the string tension as  $a_\sigma^{-1} [\text{GeV}] = 0.420 / \sqrt{\Sigma}$ .

### Ground state domination

The question of how to extract the ground state meson decay constant has been discussed quite extensively over the last years. The problem is described in section 2.5. Here, we summarize what is known in particular for mesons in the static approximation.

Following the original suggestion of Eichten [75] to compute  $\hat{F}^{\text{stat}}$ , it was noted by Boucaud et al. [94], that when one employs the static approximation, the statistical fluctuations increase rapidly with the euclidean time separation  $x_0$ . Therefore, with local operators one never observes a significant plateau in the effective mass. For that reason, they could only give an upper bound for the decay constant.

Subsequently, nontrivial wave functions were used [45, 18, 19] and  $\hat{F}^{\text{stat}}$  could first be estimated in [18, 19]. Quite some effort went into the construction of good wave functions for static-light mesons. Nevertheless, in all computations that have been done so far, one sees only relatively short plateaus in the effective masses. Ref. [96] stimulated the discussion on this point. At present the best solution to the problem is given in ref. [95]. There, the smearing wave function is determined through the diagonalization of a matrix correlation function. One thus obtains an optimal wave function out of a space of linear combinations of a number of basis functions. As a

result, out of all computations, the plateaus in the effective masses are longest and most convincing in ref. [95]. Unfortunately, only a result at one value of  $a$  is presently published with that method.

A point of discussion is also how to fit the two correlation functions  $C^{I,I}$  and  $C^{I,loc}$  in order to extract the matrix element of the local axial vector current. The analysis of refs. [95, 82] is based on a combined fit to  $C^{I,I}$  and  $C^{I,loc}$ . The appropriate range of the fits is determined from their  $\chi^2$ . Since a large correlation matrix has to be determined from a quite limited statistical ensemble, this criterion may be misleading[43, 97].

The other groups determine the (linearly divergent) binding energy  $\tilde{M}_P$  from the correlators  $C^{I,I}$ , where  $I$  labels the smearing wave function. These correlation functions have a positive spectral representation and the corresponding effective mass is easy to interpret. Also, because it is the correlation of two smeared fields, the unwanted excited states are more strongly suppressed than in  $C^{I,loc}$ . The analysis then proceeds in the following way: either one uses the binding energy as extracted from  $C^{I,I}$ , performs a fit to  $C^{I,loc}$  constraint by this energy and then obtains the decay constant from the amplitudes in the two fits[19] or one determines the height of the plateau of the ratio  $C^{I,loc}/C^{I,I}$  and combines that with the amplitude of the fit to  $C^{I,I}$ . For further variations on the theme, see ref. [43, 44]. Concerning this analysis method, one may argue[82] that the determination of the binding energy from  $C^{I,I}$  is somewhat uncertain because there are larger statistical errors in  $C^{I,I}$  than in  $C^{I,loc}$ .

Altogether, some amount of ambiguity remains and one may suspect that some of the published results have an underlying systematic error which might be even as large as the statistical error.

We note, however, that there are nontrivial checks on the results. In particular, at  $\beta = 6.0, c_{SW} = 0$ , there are five computations [18, 19, 66, 43, 82]. Ref. [66] finds that the fits in [18] started somewhat early, introducing a small systematic error. Ref. [43] extends the calculation of ref. [19]. Therefore, we compare [66, 43, 82]. The interesting point is that three different types of wave functions were used. Refs. [66, 82] used a wave function which is a three-dimensional cube for the light quark, implemented in Coulomb gauge. The sizes of the cubes were 5–7 lattice spacings[66] and 9 lattice spacings[82]. In obvious notation we label them by  $C5 - C9$ . Ref. [43] used two different, gauge covariant, wave functions. One has an approximately gaussian shape (' $G$ ') and the other one an approximately exponential shape (' $E$ '). We can compare the results from the three different wave functions directly at one value of the light quark hopping parameter  $K = 0.1540$ . The results quoted are  $\langle 0|\bar{q}_h\gamma_0\gamma_5q_l(0)|P \rangle_G = 0.36(3)$ ,  $\langle 0|\bar{q}_h\gamma_0\gamma_5q_l(0)|P \rangle_E = 0.37(2)$  [43] and  $\langle 0|\bar{q}_h\gamma_0\gamma_5q_l(0)|P \rangle_{C5} = 0.41(5)$ ,  $\langle 0|\bar{q}_h\gamma_0\gamma_5q_l(0)|P \rangle_{C7} = 0.38(3)$  [66]. So the decay constants are in good agreement for these four different wave functions. Ref. [82] obtains a somewhat low value  $\langle 0|\bar{q}_h\gamma_0\gamma_5q_l(0)|P \rangle_{C9} = 0.31(4)$  due to the analysis method discussed above. Moreover,

it is interesting to note that the systematic effect that arises from a fit to  $C^{G,loc}(x_0)$  at too small a value of  $x_0$  is to decrease the value of the decay constant, while for  $C^{E,loc}(x_0)$  this results in an overestimate of the decay constant. So the agreement that is found at large values of  $x_0$  is nontrivial and suggests that  $x_0$  is large enough in the analysis of ref. [43]. Also in the computations with the action of Sheikholeslami and Wohlert[46, 66], two different wave functions are seen to give consistent results at  $\beta = 6.0$ . These consistency checks indicate that the problem of contaminations from excited states is not too severe.

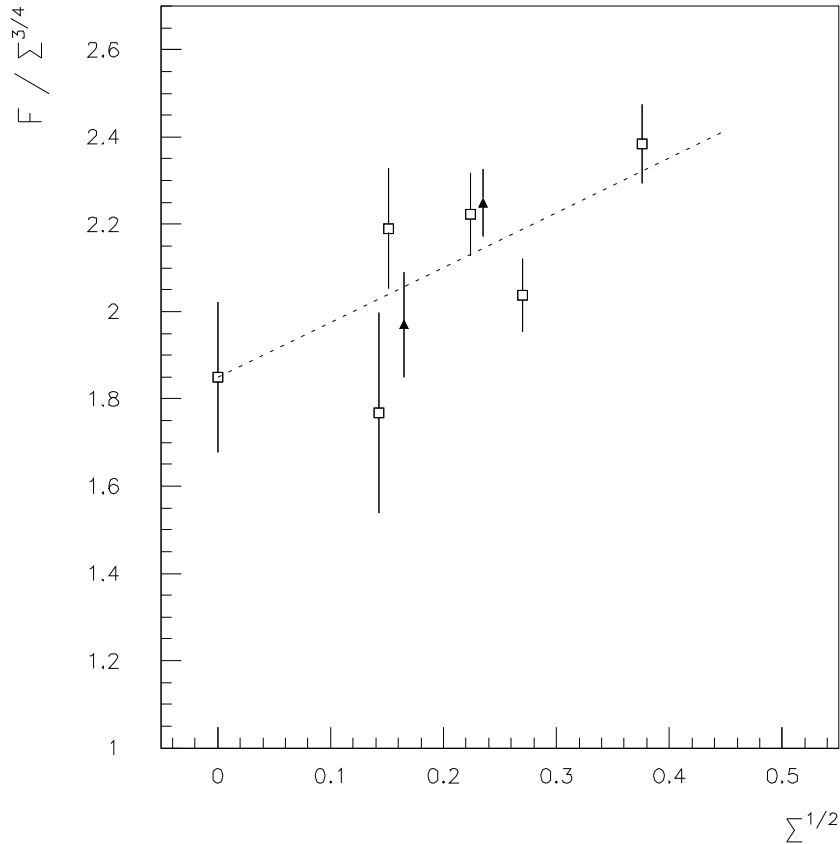


Figure 10:  $\hat{F}^{\text{stat}}$  in units of the string tension as a function of the lattice spacing. Data of refs. [43, 95, 66, 82, 46] are shown and have been combined, when they were available at overlapping values of the lattice spacing. Open boxes correspond to the Wilson action and filled triangles to the improved action.

**Finite size effects** of  $\hat{F}^{\text{stat}}$  were investigated in refs. [43, 95]. We can already infer from fig. 6, that they should be negligible once  $L\sqrt{\Sigma} = 3$  (the figure shows that the finite size effects decrease as the heavy quark mass increases). This is in agreement with the study of refs. [43, 95].



**Lattice spacing effects** are a significant remaining source of a systematic error. In order to investigate it, we consider  $\hat{F}^{\text{stat}}$  in units of the string tension. The data of refs. [43, 95, 66, 82, 46] is shown in fig. 10. Here, the renormalization constant was obtained by using the perturbative expansion in terms of  $\tilde{\alpha}$ . Overall, the lattice spacing dependence appears not to be very strong. This statement refers precisely to the ratio  $\hat{F}^{\text{stat}}/\Sigma^{3/2}$ : In most of the early computations, the mass of the  $\rho$ -meson was used to set the scale. Due to the strong dependence of  $M_\rho/\sqrt{\Sigma}$  (with  $c_{SW} = 0$ ) on the lattice spacing, there is a strong dependence on  $a$  when the scale is set through  $m_\rho$ . This explains why the earlier computations, working at  $\sqrt{\Sigma} > 0.2$  and setting the scale through  $m_\rho$ , obtained quite large values of  $\hat{F}^{\text{stat}}$  (see table 2).

The data with  $c_{SW} = 0$  is extrapolated to zero lattice spacing as shown by the dashed line:  $\hat{f}^{\text{stat}}/\sigma^{3/4} = 1.85(17)$ . One can see at a glance that the fit does not have a good  $\chi^2$ . However, it is obvious from the figure that this is not due to deviations from the assumed linear dependence on the lattice spacing. Rather, it is due to the scatter of the data itself. The most likely explanation for the scatter is incomplete ground state domination in some of the data points. A systematic error of the order of half of the statistical errors could account for the scatter in fig. 10.

Since a better procedure is lacking at the moment, we account for this scatter by taking in addition to the statistical error of the extrapolated value a systematic error of the same size. In the future, this systematic error should be removed by a further improvement of the trial wave functions.

We further estimate the error of the missing higher order terms in the perturbative expansion of  $Z_{stat}$  in the following way. We allow for a 2-loop term  $5 \tilde{\alpha}$  in  $Z_{stat}$  (a coefficient as large as five is certainly a conservative estimate). With this term the whole extrapolation is repeated. The change in the extrapolated value gives the systematic error  $\pm 0.08$ .

The data with the improved action ( $c_{SW} = 1$ , triangles) are fully consistent with the  $c_{SW} = 0$  points. We must, however, remember that in the comparison between the two sets of data an  $O(\tilde{\alpha}^2)$ -uncertainty exists and the  $a$ -dependence could be quite different. We should only compare the extrapolated values. With the two points at hand, such an extrapolation is not possible<sup>16</sup>.

Altogether we obtain

$$\hat{f}^{\text{stat}}/\sigma^{3/4} = 1.85(17)(17)(8) . \tag{4.6}$$

As in the case of  $f_D$ , it is better to change from a prediction in units of the string tension to one in units of  $f_\pi$ , since a phenomenological value for the string tension is

---

<sup>16</sup> Clearly, there is no evidence that the  $a$ -dependence in *this* observable is reduced compared to  $c_{SW} = 0$ .

based on assumptions. Furthermore, one may hope that effects of dynamical fermions are reduced when one normalizes to a decay constant. So we combine  $\hat{f}^{\text{stat}}/\sigma^{3/4}$  with  $f_\pi/\sqrt{\sigma} = 0.270(12)$  to

$$\frac{\hat{f}^{\text{stat}}}{f_\pi^{3/2}} \times (0.132 \text{ GeV})^{3/2} = 0.63(6)(6)(3)\text{GeV}^{3/2}. \quad (4.7)$$

This corresponds to  $f_B = 276(26)(24)(12) \text{ MeV} + O(m_N/m_B)$ . The errors quoted are (in order of appearance) the statistical errors including the extrapolation, the systematic error due to possible contaminations by excited states, and a  $5\tilde{\alpha}^2$  term in the renormalization. (For the latter, it is not justified to assume a cancellation between the higher orders in  $Z_{\text{stat}}$  and  $Z_A$  because these renormalizations are of quite different origin.)

We may also change to physical units through the mass of the  $\rho$ -meson. Here, the extrapolation of fig. 5 resulted in  $m_\rho/\sqrt{\sigma} = 1.81(4)$ . Therefore,

$$\frac{\hat{f}^{\text{stat}}}{m_\rho^{3/2}} \times (0.77 \text{ GeV})^{3/2} = 0.51(5)(5)(2)\text{GeV}^{3/2} \quad (4.8)$$

is a further estimate corresponding to  $f_B = 224(22)(21)(10) \text{ MeV} + O(m_N/m_B)$ .

The difference between these two estimates is most likely an effect of the quenched approximation[89]. Consequently, the difference between eq. (4.7) and eq. (4.8) should once again be regarded as a systematic error.

## 4.2 Mass Dependence

In order to get an estimate of the terms of order  $O(m_N/m_B)$ , one may examine the mass dependence of the decay constant in the mass region around the mass of the D-meson[43, 81, 82, 46, 44, 67]. We do not consider the results of [43, 81] further at this point, because they were (partly) influenced by data with contaminations from excited states. In addition, the subsequent simulations are more precise.

Ref. [82] uses the normalization eqs. (2.22,2.25) for the axial vector current. At a fixed value of the lattice spacing, they observe that  $\hat{F}(M_P)$  for  $m_P = M_P/a = 1\text{GeV} - 3\text{GeV}$  joins smoothly with  $\hat{F}^{\text{stat}}$  obtained at that value of the cutoff. This is interpreted as showing that this normalization is the correct one in the sense of having small  $a$ -effects. This behavior at a fixed value of  $a$  is, however, automatic and is not necessarily connected to a reduction of  $a$ -effects for intermediate values of the mass. Rather, with this normalization, the expression for  $\hat{F}(M_P)$  becomes identical to  $\hat{F}^{\text{stat}}$  if one takes the mass of the quark in lattice units to infinity (apart from the renormalization

constants that differ slightly). Therefore,  $\hat{F}(M_P)$  automatically joins smoothly with the static point. Fig. 8 shows that strong  $a$ -effects are present when this normalization is used. These effects are also visible in fig. 5.18 of ref. [82]. We conclude that the belief that an application of eqs. (2.22,2.25) essentially eliminates the dependence on  $a$  in the difficult region where  $m_h$  becomes close to  $a^{-1}$  is not justified.

Instead, one needs to extrapolate[44] to  $a = 0$  at a fixed value of  $m_P$  as it is shown in fig. 8 for the case of the D-meson. This both requires systematic calculations at different values of the bare coupling and increases the statistical error of the final result. However, the latter is necessary, since it is only in this way that the errors due to the discretization are covered. Comparing different normalization prescriptions or results from different actions is indicative at most. It can not replace the systematic study of the  $a$ -dependence with one action and one normalization condition.

We have supplemented the extrapolations of [44] with the raw data of [82, 67]. The extrapolations are illustrated in fig. 11 for the largest and the smallest value of the mass of the heavy quark that was used. All that was said in section 3.3 remains true for these other values of the mass. We only include the points with  $\sqrt{\Sigma} \sim 0.4$  at the smallest values of the mass. This corresponds to a cut on the mass of the heavy quark in lattice units of about  $m_h a < 3/4$ .

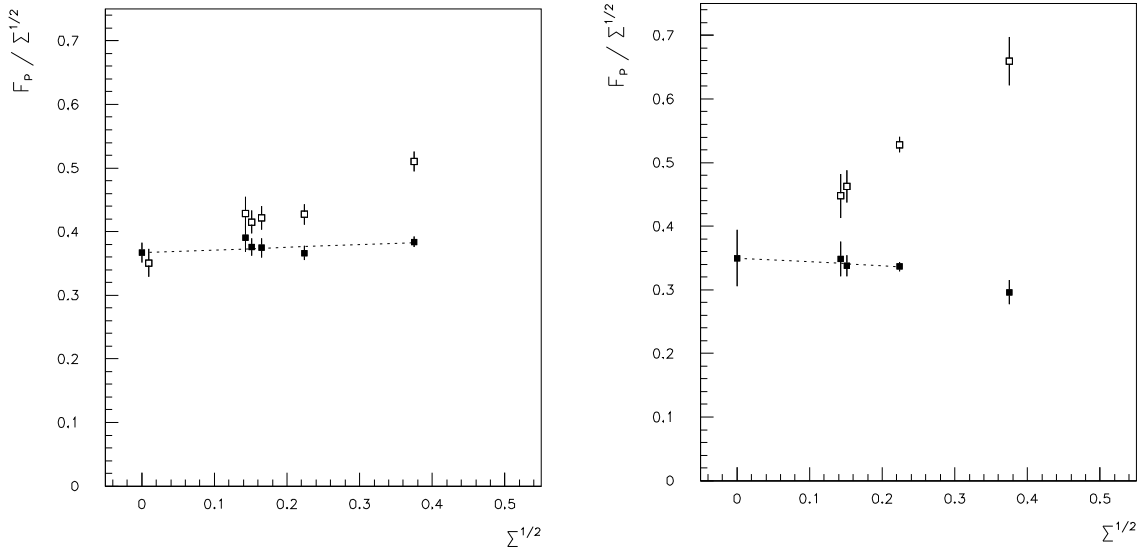


Figure 11: The lattice spacing dependence of HL-decay constants. Data points as in fig. 8.

Changing again to a prediction in terms of  $f_\pi$ , we finally arrive at the mass-dependence

of  $\hat{f}(m_P)$  depicted in fig. 12.

### 4.3 Interpolation

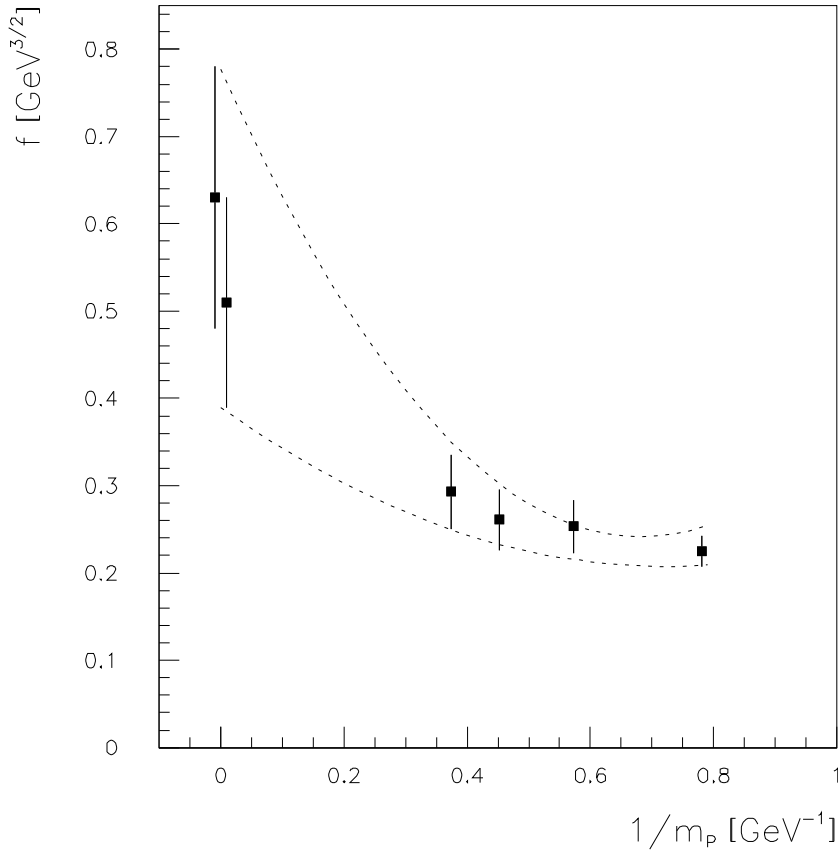


Figure 12:  $\hat{f}$  as a function of  $1/m_P$ . The two points at  $1/m_P = 0$  represent eq. (4.7) and eq. (4.8). All data has been extrapolated to the continuum allowing for a linear dependence on the lattice spacing.

In principle, we would now like to fit the results at finite values of  $m_P$  together with the result in the static approximation to a power series in  $1/m_P$ . Unfortunately, we have significant systematic errors (included in fig. 12), in particular for the result in the static approximation. Thus, it is not appropriate to perform such a fit. We just connect the upper and the lower ends of the error bars with functions  $\hat{f}(m_P) = c_0 + c_1 m_P^{-1} + c_2 m_P^{-2}$  instead.

At  $m_P = m_B$  we read off from the error band

$$f_B \equiv f_{B_d} = 180(46) \text{ MeV} . \quad (4.9)$$

One may compare this result to [46]  $f_B/f_\pi \times 132\text{MeV} = 186_{-21}^{+35}\text{MeV}$ , a value obtained with the improved action at one value of the lattice spacing  $a_\sigma^{-1} = 2.7\text{GeV}$ .

The value quoted here for  $f_B$  is obtained in the quenched approximation. The discussion in section 3.5 suggests that a similar value would result in full QCD.

Finally, the columns 3 of table 1 and table 2 may be summarized to

$$f_{B_s}/f_{B_d} = 1.10 - 1.18 . \quad (4.10)$$

#### 4.4 Comparison to QCD Sum Rule Estimates

There are a number of QCD sum rule (SR) computations of HL decay constants. These results are summarized in table 3 and are compared to the lattice gauge theory results in the quenched approximation.

Ref.	Method	$f_D/f_\pi$	$f_B/f_\pi$	$f_B^{stat}/f_\pi$
[98, 99, 100]	Laplace SR	1.1 – 1.5	0.9 – 1.5	
[101, 99]	Hilbert Moments SR	1.5 – 1.9	1.1 – 1.6	
[20, 21]	Laplace SR in HQET		1.1 – 1.9	1.5 – 2.3
eqs. (3.9,4.7,4.9)	LGT quenched approximation	1.1 – 1.4	1.0 – 1.7	1.7 – 2.5

Table 3: Estimates for HL decay constants.

We do not want to discuss details of the sum rule approach here. The interested reader may, for instance, consult the recent review ref. [102]. We point out, however, that the error estimates in table 3 are obtained from a variation of the input parameters. They do not include uncertainties due to the truncation of the operator product expansion or the question of the applicability of perturbation theory in the regime where it is used. The latter question is a particularly relevant one, since in the limit of a large heavy quark mass, the only relevant dynamical scale is the r.m.s.–radius of the light quark wave function. At such a low energy scale, it is very questionable whether perturbation theory can be applied.

An essential difference between the QCDSR estimates and the lattice gauge theory approach is that the latter can be systematically improved. We elaborate further on this point in the following.

#### 4.5 Potential Improvements

The present best estimates for  $f_B$  still contain a significant uncertainty. As we have explained in the introduction, the value of  $f_B$  is very important in the phenomenology

of the CKM–matrix. A higher precision is clearly desirable.

To this end, it is important to note that the overall computational effort that went into eq. (4.9) is quite small, when one takes a few months on today's massively parallel computers as a scale. Nevertheless, the investigations that have been done, have led to eq. (4.9) and, even more important, a semiquantitative understanding of the different sources of systematic errors (it goes without saying that the mean values have changed due to this). We therefore have a reasonable understanding of how to reduce the errors further.

In order to estimate what can be done realistically, let us assume that a parallel computer performing at 20 Gflops is accessible to a group of physicists for a good fraction of the time.

On such a computer with the existing algorithms, the computation of all correlation functions on one configuration of  $32^4 \times 96$  points at  $\sqrt{\Sigma} = 0.1$  takes roughly 6 hours. Therefore, one can obtain data points for figs. 8, 11 which have the average precision seen in the plots and which are at a 30-40% smaller value of the lattice spacing. This enables one to add points at masses as high as about 4 GeV in fig. 10 with the present precision. At the same time, one can reduce the errors of the points in the range up to 4 GeV because a new point, closer to the continuum, is added in each extrapolation<sup>17</sup>. In addition, the values in the static approximation can be significantly improved by reducing the uncertainties due to contributions by excited states. The latter point is already being addressed at Fermilab[103].

Combining this information, an overall reduction of the error of  $f_B$  (within the quenched approximation) by a factor of 2 seems plausible within a period of a year or two.

---

<sup>17</sup> It would also be useful to add points at  $\sqrt{\Sigma} \sim 0.3$  to study the  $a$ -dependence further. Note that we assume that the computations are performed at  $\sqrt{\Sigma} L \sim 3$ . With increased precision, the size of finite size effects must be checked, of course. This does not pose a problem since it can be done at a relatively large value of the lattice spacing.

## 5. B-Parameter

In the Standard Model, the mixing of  $B_0$  and  $\bar{B}_0$  is mediated by box diagrams with two  $W$ -boson exchanges. This corresponds to a short distance operator  $O^{\Delta b=2}$ , which in the continuum and at distance scales that are large compared to the interaction range of the weak interaction has the form

$$O^{\Delta b=2}(x) = (\bar{d}(x)\gamma_\mu(1 - \gamma_5)b(x))(\bar{d}(x)\gamma_\mu(1 - \gamma_5)b(x)) . \quad (5.1)$$

Its matrix element is conventionally denoted by

$$B_B^{RGI} = \alpha_s(\mu)^{-6/33} B_B(\mu) \quad (5.2)$$

with

$$\frac{8}{3} B_B(\mu) f_B^2 M_B^2 = \langle B_0 | O^{\Delta b=2}(0) | \bar{B}_0 \rangle , \quad (5.3)$$

and  $\mu$  denoting the renormalization scale. In the lattice regularization (Wilson action), the operator  $O_{lat}^{\Delta b=2}(0)$  is given to lowest order in  $\alpha$  by the naive operator eq. (5.1). To first order in  $\alpha$ , it receives admixtures from operators of the same flavor but different chiral structure[104]. This mixing is possible because of the breaking of chiral symmetry in the Wilson formulation and has been taken into account to first order in  $\alpha$  so far.

The B-parameter eq. (5.3) at scale  $\mu = a^{-1}$  can be computed directly from the ratio of three-point and two-point correlation functions

$$\frac{\sum_{\vec{x}} \sum_{\vec{y}} \langle \mathcal{M}(x) O_{lat}^{\Delta b=2}(0) \mathcal{M}^\dagger(y) \rangle}{8 \sum_{\vec{x}} \langle \mathcal{M}(x) A_0^{b,d} \rangle \sum_{\vec{y}} \langle \mathcal{M}(y) A_0^{b,d} \rangle} \longrightarrow B_B(\mu = a^{-1}) , \quad (5.4)$$

where  $\mathcal{M}$  denotes any interpolating field for a  $b\bar{d}$  meson. In eq. (5.4) the time separations  $-x_0$  and  $y_0$  are to be taken large enough such that only the lowest state contributes, i.e. such that one obtains the on-shell matrix element. Analogously to the case of two-point functions, this condition is checked by looking for a joint plateau in  $x_0$  and  $y_0$  over some range of these variables. Such a plateau appears to be reached already at moderate  $-x_0, y_0$  [78, 106, 81]. Presumably, the reason is that the contributions of excited states to eq.(5.4) are similar to the ground state contribution.

Abada et al.[81] have computed the B-parameter for meson masses between 1.5 GeV and 3.5 GeV and with a cutoff  $a^{-1} \sim 3.7$  GeV. Since the mass dependence is very weak, an extrapolation to  $m_B$  seemed justified. Also the B-parameter for the  $D$  meson was quoted:

$$B_D^{RGI} = 1.05(8) \quad (5.5)$$

$$B_B^{RGI} = 1.16(7). \quad (5.6)$$

The B-parameters turned out to depend only weakly on the mass of the light quark in the meson. For the ratio of the B-parameter of the strange meson to that of the nonstrange meson ref. [81] obtained (independently of the mass of the heavy quark)

$$B_{P_s}/B_{P_d} = 1.02(2) . \tag{5.7}$$

We point out that the above quoted errors do not contain the  $O(\alpha^2)$  uncertainty in the renormalization (which includes mixing) of the operator. An estimate of the  $O(a)$  terms in this quantity has not been given either. As discussed in the previous section, the latter uncertainty needs to be studied through systematic computations at different values of the lattice spacing. Before such a study is completed, the numbers quoted in this section have to be considered as rough estimates.



## 6. The Size of $1/m_h$ Corrections to the Heavy Quark Limit

An important nonperturbative question in heavy quark physics is to determine for which values of the heavy quark mass the predictions that one obtains in the heavy quark limit, i.e. for  $m_h \rightarrow \infty$ , become accurate. Of course, this is not a question with a precise answer: if we have a quantity like  $\hat{f}$  with an expansion in the inverse heavy quark mass  $m_h^{-1}$

$$\hat{f}(m_h^{-1}) = \hat{f}^{\text{stat}}(1 + \hat{f}_1 m_h^{-1} + \dots) \quad , \quad (6.1)$$

the mass scale  $\hat{f}_1$ , that characterizes the size of the corrections is nonuniversal; it depends on the quantity considered. Nevertheless, it is of interest for applications of the HQET to see, whether – in examples – scales like  $\hat{f}_1$  are of the order of the size of the QCD scale  $\Lambda_{QCD}$  as it is frequently assumed.

Fig. 12 gives a rough estimate  $\hat{f}_1 \sim 1\text{GeV}$ . Although a number of this order has been quoted in almost all recent publications [81, 43, 82, 46], it is evident from our discussion in section 4. that  $\hat{f}_1$  has very large uncertainties. The main uncertainty is due to the present error of the static value.

Hence, it is very useful to consider a quantity for which the heavy quark limit is known. Such a quantity was first discussed in refs. [105, 81]. Besides the pseudoscalar decay constant, one also considers the vector meson decay constant  $f_V$ , which is conventionally defined as

$$\langle 0|V_\mu(0)|V \rangle = \epsilon_\mu F_V^{-1} M_V^{3/2} / \sqrt{2} \quad . \quad (6.2)$$

Here,  $V_\mu$  denotes the (renormalized) heavy light vector current,  $|V \rangle$  is a momentum zero vector meson state with polarization vector  $\epsilon_\mu$  and  $M_V$  is the mass of the vector meson. Due to the spin symmetry, the combination  $U(M) = F_V F_P / M$ , with  $M = (M_P + 3M_V)/4$ , becomes one in the heavy quark limit[93]:

$$U(M) \equiv F_V F_P / M = (1 + \frac{2}{3\pi} \alpha(M) + \dots)(1 + U_1/M + \dots) \quad . \quad (6.3)$$

Since  $U(M)$  is the ratio of two very similar quantities, the finite lattice spacing effects in  $U(M)$  may be reduced compared to the ones in  $\hat{f}$  and also excited state contributions are expected to be less of a problem. Using masses around the mass of the  $D$ -meson, Baxter et al.[46] determined  $U(M)$  with the improved action. Interpreting their results in terms of  $U_1$ , one has  $U_1 \sim 0.5\text{ GeV}$  in agreement with the rough results[105, 81] that were obtained with the Wilson action.

So scales of about 0.5 GeV to 1 GeV are found for the coefficients of the  $1/m_h$  terms in the two known examples. This suggests that the heavy quark limit only gives the correct picture for charm quarks on a qualitative level, while it appears to be a quite reasonable approximation for  $b$ -physics. In the important application of  $b \rightarrow c$

transitions, corrections of order  $O(1/m_c)$  may be of practical relevance. Although these conclusions are obtained entirely in the quenched approximation, it is to be expected that this *qualitative* result also holds true for full QCD.

Since the  $1/m_c$ -corrections are nonuniversal, the simple examples considered above give us only a rough idea about the quality of the approximations for different processes. In the end, the relevant quantities have to be determined directly from QCD.

## 7. The $B - \bar{B}$ Threshold, String Breaking and Hybrid Mesons

Following ref. [43], we now review, how to obtain information about the breaking of the QCD-string from the binding energy  $\tilde{M}_p$  of a static B-meson computed in the quenched approximation. Moreover, it is of interest to compare the  $B - \bar{B}$  threshold with the lowest level of a hybrid  $b - \bar{b}$  meson[107, 108] in order to estimate whether such  $b - \bar{b}$  mesons are broad or narrow resonances. This is done at the end of the section.

In full QCD simulations, the breaking of the QCD string, i.e. the flattening of the heavy quark potential at large distances, has been sought after for some time. No effect was found in the most serious effort [58]. In the following, we estimate the distance  $r_b$ , where the full QCD potential flattens off using only quantities calculated in the quenched approximation [43].

Consider a large Wilson loop  $W(\vec{r}, x_0)$ , with  $x_0 \gg r$ , in full QCD. It has a representation in terms of the eigenvalues of the QCD-hamiltonian (or transfer matrix):

$$W(\vec{r}, x_0) = \sum_{n \geq 0} |c_n^W(\vec{r})|^2 \exp(-V_n(\vec{r})x_0) \quad . \quad (7.1)$$

Here,  $\exp(-aV_n(\vec{r}))$  are the eigenvalues of the transfer matrix in the corresponding charged sector of the Hilbert space: the states in this sector transform according to the  $\mathbf{3}$ -representation at position  $\vec{0}$  and according to the  $\bar{\mathbf{3}}$ -representation at position  $\vec{r}$  under gauge transformations. The same states contribute in the spectral decomposition of the correlation function of static-light meson fields  $\mathcal{M}^J(\vec{x}, x_0)$

$$\begin{aligned} H(\vec{r}, x_0) &= \langle \mathcal{M}^J(\vec{0}, x_0) [\mathcal{M}^J(\vec{r}, x_0)]^\dagger \mathcal{M}^J(\vec{r}, 0) [\mathcal{M}^J(\vec{0}, 0)]^\dagger \rangle \\ &= \sum_{n \geq 0} |c_n^H(\vec{r})|^2 \exp(-V_n(\vec{r})x_0) \quad . \end{aligned} \quad (7.2)$$

The ground state potential  $V(\vec{r}) \equiv V_0(\vec{r})$  can therefore be called a static quark potential or a static meson potential. Physically, the first interpretation is sensible at relatively

short distances, whereas the second one is the appropriate language for large distances (compared to the confinement scale). This can even be put into a quantitative relation: we expect  $|c_0^H(\vec{r})|^2 \ll |c_0^W(\vec{r})|^2$  at small distances and  $|c_0^H(\vec{r})|^2 \gg |c_0^W(\vec{r})|^2$  at large distances.

Furthermore, at large distances, the potential will approach a constant up to nonleading terms (Yukawa-type interactions), because the correlation function factorizes:

$$\log[H(\vec{r}, x_0)] = 2 \log[C^{J,J}(x_0)] + O(\exp[-m_\pi r]x_0/r) \quad . \quad (7.3)$$

Simulation results of full QCD [58] indicate that the QCD-potential is approximated rather well by the quenched potential out to relatively large distances, up to about  $r \sim 0.7fm$ . At very large distances, on the other hand, we expect that  $H(\vec{r}, t)$  is represented with some accuracy by the quenched approximation. We must switch from one correlation function to the other when using the quenched approximation, since we have to put the breaking of the string in by hand. Obviously, the quenched approximation does not give us much information about the intermediate regime.

The (in  $r = |\vec{r}|$ ) asymptotic behavior of the correlation function  $H(\vec{r}, t)$  is given by the mass in the static approximation. So one defines[43] the string breaking distance  $r_b$  by

$$V(r_b) = 2\tilde{M}_P, \quad (7.4)$$

with  $V(r)$  being the quenched potential including the self-energy term that cancels in eq.(7.4).  $r_b$  defined in this way, gives an upper bound to the distance where the potential starts deviating significantly from the form of eq.(2.34).

From the explicit parametrization of the potential eq.(2.34) one can calculate  $r_b$  in lattice units:

$$R_b = (\tilde{M}_P - \frac{1}{2}V_0)/\Sigma + \sqrt{[(\tilde{M}_P - \frac{1}{2}V_0)/\Sigma]^2 + \frac{\pi}{12\Sigma}} \quad . \quad (7.5)$$

Extending the numerical evaluation of ref. [43], we have included the data of refs. [95, 82] and extrapolated  $r_b\sqrt{\Sigma}$  linearly to the continuum (see fig. 13). The resulting value in the continuum limit is (for vanishing light-quark mass)

$$r_b\sqrt{\sigma} = 3.5(2)(2) \quad , \quad (7.6)$$

where the first error is statistical and the second is an estimate of the uncertainty due to the extrapolation form (In this case, the  $a$ -dependence is rather strong). With  $\sqrt{\sigma} \sim 420$  MeV, this corresponds to  $r_b = 1.7(2)$  fm.

Such distances are difficult to reach in a calculation of the potential including dynamical fermions. It should be noted, however, that as a result of the investigation of [43],

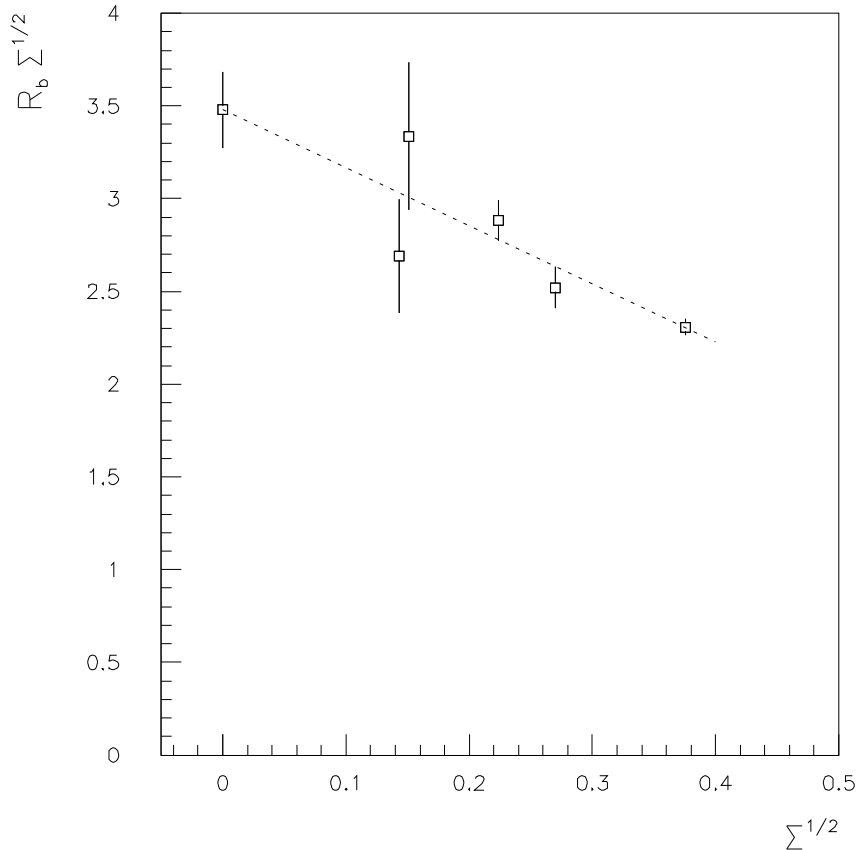


Figure 13: Continuum extrapolation of  $r_b$  for light-quark mass zero. Eq. (7.5) is used with data for  $\tilde{M}_P$  from refs. [43, 95, 82].

the screening of the potential is expected to appear at distances that are only weakly dependant on the dynamical quark mass. The mechanism can hence be studied with relatively large (dynamical) quark masses.

In the above presentation, we have translated the information that is present in the threshold energy  $2\tilde{M}_P$  into the string breaking distance  $r_b$ , where the divergent self-energy of the static quark is cancelled. In a certain approximation, to be discussed below, the difference between the  $B - \bar{B}$  threshold and the mass of a hybrid  $b - \bar{b}$  meson[108] is also free of this divergence. As the position of the  $b - \bar{b}$  energy level relative to the threshold determines the width of the  $b - \bar{b}$  resonance, this quantity is an interesting observable.

A hybrid  $b-\bar{b}$  meson is a  $b-\bar{b}$  bound state, with quantum numbers that do not occur in a naive potential model. Such “exotic” bound states are an interesting possibility due to

QCD. Describing the  $b$ -quarks through a nonrelativistic potential model, exotic states are possible through nontrivial angular momentum configurations of the gluon field which generates the potential. Such excited potentials have been computed from lattice gauge theory[107]. The nonrelativistic Schrödinger equation with those potentials can be solved and thus one gets an estimate for the energy levels of hybrid  $b-\bar{b}$  mesons. As the (excited) potential between static quarks is used, the energy levels contain (twice) the self energy of a static quark. The difference of an energy level to  $2\tilde{M}_P$  is free of this divergent contribution and represents a well defined estimate of whether the state is above or below the open  $b$  threshold. Of course, the estimate is obtained within the quenched and the potential model approximations.

Using the result of ref. [107] one estimates for the lowest exotic level in the  $b-\bar{b}$  system

$$[E_{1^{-+}} - V(r_0)]/\sqrt{\sigma} \sim 2.0 \quad (7.7)$$

and for the threshold

$$[E_{B\bar{B}} - V(r_0)]/\sqrt{\sigma} = 2\tilde{M}_P - V(r_0)/\sqrt{\sigma} = 2.5(4) \quad , \quad (7.8)$$

where we have arbitrarily normalized to  $V(r_0)$ . So, the exotic state appears to be  $\sim 200$  MeV *below* the threshold. Adding the information that the wave function at the origin is very small due to the flat potential[107], the state is expected to have a very small width. Note, however, that even within the model used here, the uncertainty is so large that a coincidence of the threshold and the hybrid level is just at the edge of the error bar.

Previously, the position of the  $B\bar{B}$  threshold relative to the mass of the hybrid meson has been estimated in the following way[107]: The difference of  $E_{1^{-+}}$  and the mass of the lowest  $b-\bar{b}$  bound state  $m_\Upsilon$  was estimated with the above model. Then the experimental value for  $2m_B - m_\Upsilon$  gives the position of the threshold relative to  $E_{1^{-+}}$ . In this way one arrives at the conclusion that the  $1^{-+}$  state is  $\sim 250$  MeV *above* the threshold.

Remaining consistently in the quenched approximation, the opposite seems to emerge, giving new hope for the existence of a narrow, interesting state. Further progress about this problem can most likely be made within the framework of non-relativistic QCD.

## 8. The Beauty Spectrum

The spectrum of bound states of a b–quark with light quarks represents one of the possible predictions of QCD. It has been explored to some extent using the static approximation. Estimates of the corrections of order  $O(m_N/m_B)$  do not exist and are in fact not of primary interest at this point, since the computations within the static approximation need considerable improvement. For any state, the self energy of the static quark must be cancelled to obtain a finite result. This is done by considering energy differences to the mass of the B–meson .

Due to the spin symmetry in the static approximation[6], there is a degeneracy of vector– with pseudoscalar mesons and axialvector– with scalar mesons. We denote the remaining splitting between scalar and pseudoscalar by  $\Delta_S$ . Of further interest is the splitting between the  $\Lambda_b$  and the  $B$ , denoted by  $\Delta_\Lambda$ . Also the first radially excited state with splitting  $\Delta_{2s}$  of the  $B$  has been investigated[95] and an estimate of the difference between the  $B_s$  and the  $B \equiv B_d$  was given[66]. We now comment on some technical points of these computations.

The computation of the mass splittings between states with different quantum numbers is straight forward in principle. i) One chooses (in addition to eq. (2.29) ) an interpolating field with the desired quantum numbers. ii) One searches for the exponential decay of the correlation functions and computes the mass splitting as the difference, or one takes the ratio of the two correlation functions directly and searches for a plateau in the effective mass of the ratio.

The scalar meson is a p-wave in the non-relativistic quark model. It is therefore natural to insert a p-wave smearing function into eq. (2.28) in order to obtain an interpolating field for a scalar meson. For gauge covariant wave functions, this can be achieved by applying a covariant derivative to the symmetric wave function. This approach was tried in ref. [43], but the correlation function was found to be very noisy. The results quoted in ref. [43] were obtained by replacing  $\gamma_0\gamma_5 \rightarrow 1$  in eq. (2.29) and using a spatially symmetric wave function, that means the lower components of the light–quark field are used to obtain the parity change relative to the pseudoscalar. Ref. [95] does obtain results with a p-wave smearing function in Coulomb gauge. Presumably, the reason is that in a fixed gauge, the detailed form of the smearing function can be chosen; ref. [95] uses the wave function of a semi–relativistic potential model for that purpose.

The interpolating field for the  $\Lambda_b$  has been chosen as[109, 43]

$$\mathcal{B}_\alpha^{I,J}(x) = \sum_{a,b,c,\beta,\gamma} \epsilon_{abc} (h^I(x))_\alpha^a (u^J(x))_\beta^b (C\gamma_5)_{\beta\gamma} (d^J(x))_\gamma^c . \quad (8.1)$$

Here a,b,c ( $\alpha, \beta, \gamma$ ) denote color (Dirac) indices. The field  $\mathcal{B}_\alpha^{I,loc}(x)$  is to be interpreted

as an extreme di-quark trial wave function for the baryon: the two light-quark fields are taken at the same point. Otherwise,  $\mathcal{B}_\alpha^{I,J}(x)$  amounts to a more general wave function ansatz. In ref. [109], the di-quark option was chosen, while ref. [43] explored both possibilities. An interesting feature of the correlation functions of  $\mathcal{B}_\alpha^{I,J}(x)$  is that the di-quark interpolating field  $\mathcal{B}_\alpha^{I,loc}(x)$  is much less effective in exciting a  $\Lambda_b$  state than the field  $\mathcal{B}_\alpha^{I,I}(x)$ , where all quarks have an independent spatial wave function[43].

Ref.	$\Delta_\Lambda$ [GeV]	$\Delta_S$ [GeV]	$\Delta_{2s}$ [GeV]	$M_{B_s} - M_{B_d}$ [MeV]	$a_\sigma^{-1}$ [GeV]
[109]	$0.72_{-0.16-0.13}^{+0.16+0}$			$71_{-13-16}^{+13+0}$	1.9
[43]	$\sim 0.6$	$\sim 0.35$			1.3 - 2.7
[95]		$\sim 0.4$	$\sim 0.4$		1.6
[66]				70 - 140	1.9

Table 4: A compilation of mass splittings as they were obtained in the *static approximation*. The last column gives the value of the cutoff.

Determining the energy of a (radially) excited state is a more difficult task. For that purpose, a matrix correlation function needs to be considered. From such a matrix correlation function, a quantity which is analogous to the local mass (cf. sect. 2.5) can be constructed and it was shown that this quantity converges exponentially (in  $x_0$ ) to the mass splitting[110]. Thus the situation is – at least in principle – the same as for the splitting between two states with different quantum numbers.

The computation of the 2S - 1S splitting in ref. [95] has not exactly been done in this way. Rather, starting from a  $2 \times 2$  matrix correlation function (where the two smearing functions are again obtained from the semi-relativistic potential model and should lead to relatively good interpolating fields for the lowest two levels), an optimal wave function was found for the ground state first. Then the correlation function was projected onto the part orthogonal to that *approximate* ground state. The excited state mass was determined from that projected correlation function. Since there always remains a small contribution from the exact ground state in the projected correlation function, one will at very large  $x_0$  determine again the mass of the ground state. Although this is in principle a problem of the computation ref. [95], we do not think that this effect is numerically important at the moment. Furthermore, it can easily be corrected in the future.

The main feature of all the computations[109, 43, 95] of the mass splittings is that the plateaus in the effective masses are less convincing than for the pseudoscalar state. So the results are less precise and it has not been possible to study systematic errors due to  $a$ -effects<sup>18</sup>. Therefore, these estimates are qualitative at the moment. Where this was done in the literature, we will quote numbers with error bars below, but we stress

<sup>18</sup> Finite volume effects have been studied within a model for  $\Delta_S$  and  $\Delta_{2s}$  [95].

that they do not include a realistic estimate of systematic errors. The results of the various investigations are listed in table 4.

In addition to the observables that we considered so far, Bochicchio et al.[109] estimated the vector – pseudoscalar splitting at order  $1/m_h$ . The computation is done starting from the static approximation and including the  $\vec{\sigma}\vec{B}$  term of eq. (2.36) perturbatively. The result at  $a_\sigma^{-1} = 1.9$  GeV is  $m_V^2 - m_P^2 = (0.19_{-0.04-0.07}^{+0.04+0})\text{GeV}^2$ , which is significantly below the experimental  $m_{B^*}^2 - m_B^2 \sim m_{D^*}^2 - m_D^2 \sim 0.55 \text{ GeV}^2$ . Lacking estimates of the systematic errors, it is premature to speculate from where this difference originates. It poses an interesting problem for future investigations.



## 9. Further Lattice Investigations

There are a number of interesting investigations of other physical observables in the context of HL hadrons. Let us mention just the ones which we believe have the potential to contribute to the analysis of experimental data as mentioned in the introduction.

Semileptonic decay form factors for  $D$ -decays have been studied [12, 13] and exploratory studies of  $B$ -decays have been performed[13]. Computations of the Isgur-Wise-function are attempted[111] and the nonperturbative amplitude for the decay  $B \rightarrow K^*\gamma$  has recently been estimated[112].

We mention these investigations for completeness. Compared to the leptonic decay constants there is scarcely a study of the systematic uncertainties available at the moment. In particular, the size of finite lattice spacing effects are not known at present, but we would like to point out that the feasibility of such computations is clearly demonstrated. Thus, there is considerable potential in these computations. An initial understanding of the systematic uncertainties of these quantities should develop within the next year or two. After that stage, these computations might represent predictions of a well-tested model, quenched QCD. As such, they might already be a valuable contribution to the analysis of experimental data.

The necessary computations in full QCD will be facilitated by what can be learned from the quenched approximation. Nevertheless, it is not possible to predict exactly when first principle calculations of these hadronic matrix elements, i.e. reliable calculations in full lattice QCD, can be done.

## 10. Summary

We have given an overview of the present status of QCD lattice simulations that involve the  $b$  quark. The discussion was centered around the most easy quantity, the vacuum-to-one-meson matrix element. That matrix element gives us the leptonic decay constant and in the case of the  $B$ -meson it is the primary unknown in the process of extracting the CKM angles from experimental data.

Unfortunately, the  $B$ -meson is particularly difficult to treat in a lattice simulation. This is simply due to the large gap in the relevant scales in the problem. These scales are i) the confinement scale which determines the physical size of a  $B$ -meson and thus is the scale that is relevant for finite size effects and ii) the mass of the  $b$ -quark itself. The latter needs to be small compared to the cutoff such that the quark can propagate without large distortions due to the finite cutoff. These two scales cannot be accommodated on today's lattices.

A way out is to consider the observables of interest in two unphysical regimes, obtaining the physical observables through a matching of the two. The first regime is the static limit  $m_b \rightarrow \infty$ . In this limit, the scale  $m_b$  itself becomes irrelevant and results can – in principle – easily be obtained. The second regime is  $m_h \sim m_c$ , where one is at the edge of the possibility of treating the heavy quark correctly while still keeping finite size effects small. We have emphasized that it is very important to systematically perform simulations with different values of the cutoff  $a^{-1}$  and fixed value of  $m_h$  in this regime and extrapolate the results to the continuum limit  $a \rightarrow 0$ . The uncertainties due to the finite cutoff can only be taken into account in this way. The necessity to extrapolate  $a \rightarrow 0$  introduces quite large errors, even in the quenched approximation. Nevertheless, it is straightforward to reduce these uncertainties using the knowledge which has been acquired over the last years.

The precise studies are still restricted to the quenched approximation. It is quite interesting, however, that a systematic comparison of full QCD results with the quenched approximation in the range  $m_h \sim m_c$  shows no effect of sea quarks with a mass of about  $m_s$ .

Other quantities like the  $B$ -parameter and mass splittings have not been studied very systematically yet. Particularly concerning the  $B$ -parameter, this deficiency needs to be filled.

In addition, we explained how one can get information on the breaking of the QCD-string from simulations in the quenched approximation by comparing the open  $B$  threshold in the static approximation with the static potential.

## A Renormalization of Vector Currents

For HL-mesons the axial vector current and the vector current have been normalized in different ways[33, 34, 35], as discussed for the axial vector current in sect. 2.4. In the case of the local vector current, the relativistic normalization is

$$V_\mu^{f,f'}(x) = Z_V(g_0^2, K_f, K_{f'}) \bar{q}_f(x) \gamma_\mu q_{f'}(x) \quad (\text{A1})$$

with the one-loop expression[31, 36, 35]

$$Z_V(g_0^2, K_f, K_{f'}) = 1 - 0.17408 \tilde{g}^2 + O(\tilde{g}^4) + O(am_f) + O(am_{f'}) . \quad (\text{A2})$$

The non-relativistic normalization of Kronfeld, Lepage and Mackenzie reads

$$V_\mu^{f,f'}(x) = \tilde{Z}_V(g_0^2, K_f, K_{f'}) \sqrt{\frac{1}{2K_f} - 3\bar{u}} \sqrt{\frac{1}{2K_{f'}} - 3\bar{u}} \bar{q}_f(x) \gamma_\mu q_{f'}(x) , \quad (\text{A3})$$

with

$$\tilde{Z}_V(g_0^2, K_f, K_{f'}) = 1 - 0.0656 \tilde{g}^2 + O(\tilde{g}^4) + O(am_f) + O(am_{f'}) . \quad (\text{A4})$$

It is claimed in the literature that in the region where  $am_f$  is of order one, the normalization eqs. (A3,A4) (and eqs. (2.22,2.25)) represent the “correct” normalization of the currents. Here, “correct” has to be interpreted as being the normalization with small lattice artifacts.

The partially conserved vector current

$$\hat{V}_\mu^{f,f'}(x) = \frac{1}{2} [\bar{q}_f(x) (\gamma_\mu - 1) U_\mu(x) q_f(x + a\hat{\mu}) + \bar{q}_f(x + a\hat{\mu}) (1 + \gamma_\mu) U_\mu^\dagger(x) q_f(x)] \quad (\text{A5})$$

has the same normalization in the two approaches, however[113].

We consider[13, 113] the ratio

$$R_V(K_f, K_{f'}) = \frac{\sum_{\vec{x}} \langle \bar{q}_{f'}(x) \gamma_k q_f(x) \hat{V}_k^{f,f'}(0) \rangle}{\sum_{\vec{x}} \langle \bar{q}_{f'}(x) \gamma_k q_f(x) \bar{q}_f(0) \gamma_k q_{f'}(0) \rangle} . \quad (\text{A6})$$

Away from the short distance lattice artifacts this gives one definition of the renormalization constant of the local current. In the relativistic normalization one obtains for this ratio

$$R_V(K_f, K_{f'}) = Z_V(g_0^2, K_f, K_{f'}) = 1 - 0.17408 \tilde{g}^2 + O(\tilde{g}^4) + O(am_f) + O(am_{f'}) , \quad (\text{A7})$$

while the non-relativistic normalization predicts a strong mass dependence

$$R_V(K_f, K_{f'}) = (1 - 0.0656 \tilde{g}^2) \sqrt{\frac{1}{2K_f} - 3\bar{u}} \sqrt{\frac{1}{2K_{f'}} - 3\bar{u}} + O(\tilde{g}^4) + O(am_f) + O(am_{f'}) \quad (\text{A8})$$

In fig. 14, the Monte Carlo data for  $R_V$  is compared to the above two expressions. It is seen that at small  $m = 1/(2K_f) + 1/(2K_{f'}) - 1/K_c$  the predictions are essentially the same. At growing quark masses, the prediction of the non-relativistic normalization deviates much further from the Monte Carlo results than the one from the relativistic normalization. In fact, the latter describes the mass-dependence very well. One also sees that the difference between the 1-loop expression for  $R_V$  and the nonperturbative results decreases significantly as the lattice spacing is reduced (from the right figure to the left, the lattice spacing changes by a factor  $\sim 0.6$ ).

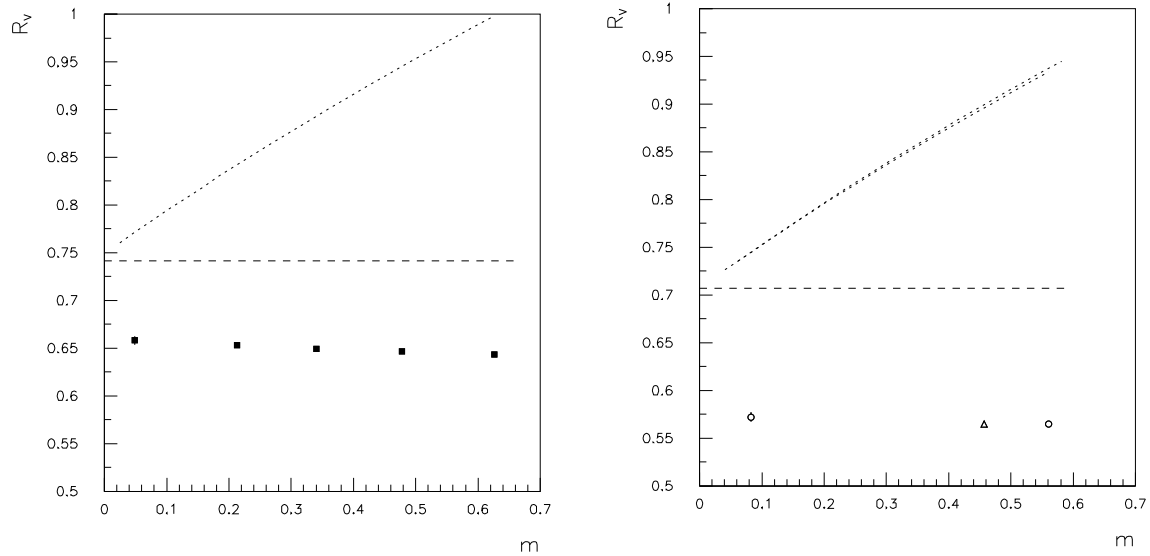


Figure 14:  $R_V$  compared to eq. (A7) (dashed line) and eq. (A8) (dotted line). The left hand figure is for  $\beta = 6.4$  [13] and the right hand figure for  $\beta = 6.0$  [113].

Finally, let us mention that for the improved action, one obtains a much better agreement of  $R_V$  with 1-loop perturbation theory. This and the fact that other nonperturbative definitions of  $Z_V$  give significantly different results[40, 29], suggests that the difference between the dashed curve and the data in fig. 14 is dominantly an  $O(a)$  lattice artifact rather than an effect of truncating perturbation theory at that order. Indeed, the numbers are in agreement with an almost linear correction in  $a$ , but does, of course, not rule out more complicated corrections.

This example shows that the nonrelativistic normalization, in general, does not reduce lattice artifacts that are due to large quark masses  $m_f a \sim 1$ . Rather, in the example, the lattice artifacts are increased compared to the relativistic normalization. We mainly conclude from this example that lattice artifacts have to be removed by systematically performing the limit  $a \rightarrow 0$ .

## Acknowledgements

I would like to thank C. Alexandrou, S. Güsken, F. Jegerlehner and K. Schilling for an enjoyable and productive collaboration during which I learned about most of the topics covered in this review.

I have profited from discussions on these topics with many colleagues. I would like to mention A. Ali, E. Eichten, J. Labrenz, M. Lüscher, G. Martinelli, O. Pène, C. Sachrajda and S. Sint.

I acknowledge furthermore the hospitality of the INT Summer Institute “Phenomenology and Lattice QCD”, Seattle, Washington, USA, where this work was started.

Moreover, my thanks go to C. Allton, Y. Iwasaki, A. Ukawa and D. Weingarten for sending me their data through electronic mail.

Above all I thank my wife, Dorothy, for her great patience and for proofreading this manuscript.

## References

- [1] N. Cabibbo, Phys. Lett. **10** (1963) 513;  
M. Kobayashi and K. Maskawa, Prog. Theor. Phys. **49** (1973) 652.
- [2] H. Leutwyler and M. Roos, Z. Phys. C25 (1984) 91.
- [3] Particle Data Group, J. J. Hernández et al., Phys. Lett. B239 (1990) 1.
- [4] L. Wolfenstein, Phys. Rev. Lett. 51 (1983) 1945.
- [5] M. Bauer, B. Stech and M. Wirbel, Z. Phys. C29 (1985) 637; C34 (1987) 103;  
N. Isgur, D. Scora, B. Grinstein and M. B. Wise, Phys. Rev. D39 (1989) 799;  
N. Isgur and D. Scora, Phys. Rev. D40 (1989) 1491.
- [6] N. Isgur and M.B. Wise, Phys. Lett. B232, (1989) 113;  
Phys. Lett. B237 (1990) 527.
- [7] M. Neubert and V. Rieckert, Nucl. Phys. B382 (1992) 97; M. Neubert, Phys. Lett. 264B (1991) 455, Phys. Rev. D46 (1992) 2212; for a summary see e.g. T. Mannel, in [8].
- [8] ECFA Workshop on a European B-Meson Factory, B-Physics Working Group Report, DESY preprint, DESY 93-151.
- [9] M.E. Luke, Phys. Lett. 252B (1990) 447
- [10] H. Albrecht et. al (The Argus Collaboration), preprint DESY 92-146, October 1992.
- [11] A. Ali and D. London, preprint DESY 93-022, February 1993.
- [12] M.Crisafulli et al., Phys. Lett. 223B (1989) 90;  
V.Lubicz, G.Martinelli and C.T.Sachrajda, Nucl. Phys. B356 (1991) 310;  
V.Lubicz, G.Martinelli, M.McCarthy and C.T.Sachrajda, Phys.Lett. 274B (1992) 415;  
C.Bernard, A.El-Khadra and A.Soni, Phys. Rev. D43 (1992) 2140;  
C.Bernard, A.El-Khadra and A.Soni, Phys. Rev. D45 (1992) 869.
- [13] A. Abada et al., preprint LPTENS 93/14.
- [14] A.F. Falk and M. Neubert, Phys. Rev. D47(1993)2965.
- [15] P. Franzini, Phys. Rep. C173 (1989) 1;  
E. A. Paschos and U. Türke, Phys. Rep. C178 (1989) 145.
- [16] J. Maalampi and M. Roos, Particle World 1 (1990) 148.

- [17] M. Lusignoli, L. Maiani, G. Martinelli and L. Reina, Univ. di Roma, Preprint n.792 (1991).
- [18] C.R. Allton et al., Nucl. Phys. B349(1991)598.
- [19] C. Alexandrou, S. Güsken, F. Jegerlehner, K. Schilling and R. Sommer, Phys. Lett. B256 (1991) 60.
- [20] M. Neubert, Phys. Rev. D45 (1992) 2451.
- [21] E. Bagan, P. Ball, V.M. Braun and H.G. Dosch, Phys. Lett. B278 (1992) 457.
- [22] K. G. Wilson, in *New Phenomena in Subnuclear Physics*, Erice 1975, Plenum, New York (1977).
- [23] For an introduction see for example  
M. Creutz, Quarks, gluons and lattices (Cambridge 1983);  
P. Hasenfratz, *Lattice Quantum Chromodynamics*, in “Schladming 1983, Proceedings, Recent Developments In High Energy Physics”, 283;  
I. Montvay and G. Münster, Quantum Fields on a Lattice, Cambridge University Press (1993) (to appear).
- [24] B. Sheikholeslami and R. Wohlert, Nucl. Phys. B 259 (1985) 572.
- [25] M. Lüscher, Comm. Math. Phys. 54 (1977) 283.
- [26] K. Symmanzik, Cutoff Dependence in Lattice  $\Phi_4^4$  Theory, Lecture given at Cargèse (1979), in *Recent Developments in Gauge Theories*, ed. G't Hooft et al. (Plenum, New York, 1980).
- [27] T. Reisz, Nucl. Phys. B318 (1989) 417.
- [28] M. Lüscher and P. Weisz, Comm. Math. Phys. 97 (1985) 59.
- [29] G. Martinelli, C.T. Sachrajda and A. Vladikas, Nucl. Phys. B 358 (1991) 212.
- [30] R. Sommer, preprint DESY 93-062, Nucl. Phys. B (in press).
- [31] L. H. Karsten and J. Smit, Nucl.Phys. B183 (1981) 103.
- [32] M. Bochicchio, L. Maiani, G. Martinelli, G. C. Rossi and M. Testa, Nucl. Phys. B262 (1985) 331.
- [33] G.P. Lepage in “*Lattice 91*”, Nucl. Phys. B (Proc. Suppl.) 26 (1992) 45.
- [34] A. Kronfeld, Nucl. Phys. B (Proc. Suppl.) 30 (1993) 445.
- [35] G.P. Lepage and P. Mackenzie, Phys. Rev. D48(1993)2250.

- [36] R. Groot, J. Hoek and J. Smit, Nucl. Phys. B237(1984)111.
- [37] G.P. Lepage and P.B. Mackenzie, Nucl. Phys. B(Proc. Suppl.) 20 (1991) 173.
- [38] M. Lüscher, R. Sommer, P. Weisz and U. Wolff, A Precise Determination of the Running Coupling in the SU(3) Yang-Mills Theory, DESY 93-114 (1993).
- [39] G. Parisi, *in*: High-Energy Physics — 1980, XX. Int. Conf., Madison (1980), ed. L. Durand and L. G. Pondrom (American Institute of Physics, New York, 1981.)
- [40] G. Heatlie, G. Martinelli, C. Pittori, G.C. Rossi and C.T. Sachrajda, Nucl. Phys. B352 (1991) 266.
- [41] S. Güsken in proceedings of the 1989 International Symposium “*Lattice '89*”, Nucl. Phys. B (Proc. Suppl.) 17 (1990) 361
- [42] S. Güsken, U. Löw, R. Sommer, K. Schilling, K.-H. Mütter and A. Patel, Phys. Lett. B227 (1989) 266.
- [43] C. Alexandrou, S. Güsken, F. Jegerlehner, K. Schilling and R. Sommer, preprint PSI-PR-92-27; Nucl. Phys. B (in press).
- [44] C. Alexandrou, S. Güsken, F. Jegerlehner, K. Schilling and R. Sommer, preprint DESY 93-179.
- [45] E. Eichten, G. Hockney, and H. B. Thacker, Nucl. Phys. B (Proc. Suppl.) 20 (1991) 500.
- [46] R.M. Baxter et al. Edinburgh preprint 93/526.
- [47] P. Bacilieri et al., Nucl. Phys. B317 (1989) 509.
- [48] New, unpublished results from the APE-collaboration, do indeed show plateaus at large values of  $x_0$ . I thank Guido Martinelli for communicating these findings prior to publication.
- [49] S. Duane, A.D. Kennedy, B.J. Pendleton and D. Roweth, Phys. Lett. B195 (1987) 216.
- [50] S. Gupta, A. Irbäck, F. Karsch and B. Petersen, Phys. Lett. B242 (1990) 437.
- [51] D. Toissant, Nucl. Phys. B (Proc. Suppl.) 26 (1992) 3.
- [52] A. Ukawa, Nucl. Phys. B (Proc. Suppl.) 30 (1993) 1.
- [53] The APE group, Phys. Lett. B 214, Phys. Lett. B258 (1991) 195, Nucl. Phys. B (Proc. Suppl.) 26 (1992) 399, Nucl. Phys. B378 (1992) 616.



- [54] F. Butler, H. Chen, J. Sexton, A. Vaccarino and D. Weingarten, Phys. Rev. Lett. 70(1993) 2849.
- [55] C.W. Bernard, M.F.L. Golterman, Phys. Rev. D46(1992)853; S.R. Sharpe, Phys.Rev.D46(1992)3146.
- [56] M. Lüscher, Nucl. Phys. B180 (1981) 317.
- [57] G.S. Bali and K. Schilling, Phys. Rev. D46 (1992) 2636; the values quoted here have been reanalysed by G. Bali using eq.(2.34).
- [58] K.D. Born *et al.*, Nucl. Phys. B (Proc. Suppl.) 20 (1991) 394, Nucl. Phys. B (Proc. Suppl.) 26 (1992) 268.
- [59] C.R. Allton *et al.* Edinburgh preprint 92/507.
- [60] S. Aoki, M. Fukugita, N. Ishizuka, Y. Kuramashi, H. Mino, M. Okawa, A. Ukawa and T. Umemura, unpublished study of finite size effects in hadron masses; talk by A. Ukawa at Schloss Ringberg 1992.
- [61] S. Cabasino *et al.*, Phys. Lett. B258 (1991) 202; P. Bacilieri *et al.*, Nucl. Phys. B343 (1990) 228.
- [62] R. Gupta *et al.*, Phys. Rev. D43 (1991) 2003.
- [63] K.M. Bitar *et al.*, Nucl. Phys. B (Proc. Suppl.) 20 (1991) 362.
- [64] N. Ishizuka *et al.*, Nucl. Phys. B (Proc. Suppl.) 26 (1991) 284
- [65] S. Sharpe, Nucl. Phys. B (Proc. Suppl.) 26 (1992) 197.
- [66] C.R. Allton *et al.*, preprint LPTENS 93/12.
- [67] C.R. Allton *et al.* (the APE group), private communication by C.R. Allton.
- [68] G.P. Lepage and B.A. Thacker in “*Field Theory on the Lattice*”, Nucl. Phys. B (Proc. Suppl.) 4 (1988) 199.
- [69] C. Davies and B. Thacker in “*Lattice 91*”, Nucl. Phys. B (Proc. Suppl.) 26 (1992) 375 and 378.
- [70] G. Martinelli, L. Maiani and C. Sachrajda, Nucl. Phys. B368 (1992) 281.
- [71] P. Mackenzie, Nucl. Phys. B (Proc. Suppl.) 30 (1993) 35.
- [72] Proceedings of “*Lattice 93*”, to appear in Nucl. Phys. B (Proc. Suppl.).
- [73] Ph. Boucaud, C. L. Lin, and O. Pene, Phys. Rev. D40 (1989) 1529 + erratum; Ph. Boucaud, J. P. Leroy, J. Micheli, O. Pene, and G. C. Rossi, CERN preprint CERN-TH-6599-92.

- [74] E.Eichten and B. Hill, Phys.Lett.B240(1990)193.
- [75] E. Eichten, in *Field Theory on the Lattice*, Nucl. Phys. B (Proc. Suppl.) 4 (1988) 147.
- [76] E. Eichten and F. Feinberg, Phys. Rev. D 23 (1981) 2724.
- [77] K. M. Bitar et al., preprint FSU-SCRI-93-110.
- [78] C. Bernard, T. Draper, G. Hockney and A. Soni, Phys. Rev.D38(1988)3540.
- [79] M.B. Gavela et al., Nucl. Phys. B306 (1988) 677;  
M.B. Gavela et al., Phys. Lett. 206B (1988) 113.
- [80] T.A. De Grand and D.R. Loft, Phys. Rev. D38 (1988) 954.
- [81] A. Abada et al, Nucl. Phys. B376 (1992) 172.
- [82] C. Bernard, J. Labrenz, and A. Soni, University of Washington preprint UW/PT-93-06.
- [83] H. Hamber, Phys. Rev. D39 (1989) 896.
- [84] C. Alexandrou, S. Güsken, F. Jegerlehner, K. Schilling, and R. Sommer, Nucl. Phys. B374 (1992) 263.
- [85] see e.g. J. Gasser and H. Leutwyler, Phys. Rep. C87 (1982) 77.
- [86] C. Michael and M. Teper, Nucl. Phys. B314(1989)347.
- [87] G.S. Bali, et al. (UKQCD–coll.), Phys. Lett. B309 (1993) 378.
- [88] C. Bernard, J. Labrenz and A. Soni, Nucl. Phys. B (Proc. Suppl.) 20 (1991) 488.
- [89] F. Butler, H. Chen, J. Sexton A. Vaccarino and D. Weingarten, preprint IBM/HET 93-3. We would like to thank D. Weingarten for communicating preliminary numbers to us prior to publication.
- [90] The euclidean staggered fermion action is discussed e.g. in H.S. Sharatchandra, H.J. Thun and P. Weisz, Nucl. Phys. B192 (1981); it is based on the hamiltonian formulation given in L. Susskind, Phys. Rev. D16 (1977) 3031.
- [91] G. Kilcup, private communication.
- [92] A. Borelli, R. Frezotti, E. Gabrielli and C. Pittori, CERN preprint TH-6587 (1992).

- [93] E. V. Shuriak, Nucl. Phys. B198 (1983) 83;  
M. A. Shifman and M. B. Voloshin, Sov. J. Nucl. Phys. 45 (1988) 292;  
H. D. Politzer and M. B. Wise, Phys. Lett. B206 (1988) 681; Phys. Lett. B208 (1988) 504;  
X. Ji and M.J. Musolf, Phys. Lett. B257 (1991) 409;  
D.J. Broadhurst and A.G. Grozin, Phys. Lett. B274 (1992) 421;  
M. Neubert, Phys. Rev. D46 (1992) 1076.
- [94] Ph. Boucaud, O. Pene, V.J. Hill, C.T. Sachrajda and G. Martinelli, Phys. Lett. 220B (1989) 219.
- [95] A. Duncan et al., Nucl Phys. B(Proc. Suppl.)30 (1993) 433;  
A. Duncan, E. Eichten and H. Thacker, Phys. Lett. B303 (1993) 109.
- [96] S. Hashimoto and Y. Saeki, Hiroshima University preprint HUPD-9120 and Nucl. Phys. B (Proc. Suppl.) 26 (1992) 381.
- [97] C. Michael, Liverpool Preprint LTH 321.
- [98] T. M. Aliev and V. L. Eletsky, Sov. J. Nucl. Phys. 38 (1983) 936.
- [99] S. Narison, Phys. Lett. B198 (1987) 104.
- [100] L. J. Reinders, H. Rubinstein and S. Yazaki, Phys. Lett. B104 (1981) 305;  
Phys. Rep. C127 (1985) 1;  
L. J. Reinders, Phys. Rev. D38 (1988) 947.
- [101] C. A. Dominguez and N. Paver, Phys. Lett. B197 (1987).
- [102] P. Colangelo, G. Nardulli and N. Paver in [8].
- [103] E. Eichten in the Proceedings of “Lattice 93”, to appear in Nucl. Phys. B (Proc. Suppl.).
- [104] G. Martinelli, Phys. Lett. 141B (1984) 395;  
C. Bernard et al., Phys. Rev. D36 (1987) 3224.
- [105] R. Sommer, C. Alexandrou, S. Güsken, F. Jegerlehner and K. Schilling, Nucl. Phys. B (Proc. Suppl.) 26 (1992) 387.
- [106] R. Gupta, D. Daniel, G. Kilcup, A. Patel and S. Sharpe, Phys. Rev. D47 (1993) 5113.
- [107] S.J. Perantonis and C. Michael, Nucl. Phys. B 347 (1990) 854.
- [108] For a nice review see: C. Michael, in “*QCD 20 Years Later*”, eds. P.M. Zerwas and H.A. Kastrup, World Scientific, Aachen 1993.

- [109] M. Bochicchio, G. Martinelli, C. R. Allton, C. T. Sachrajda, and D. B. Carpenter, Nucl. Phys. B 372 (1992)403.
- [110] M. Lüscher and U. Wolff, Nucl. Phys. B339 (1990) 222.
- [111] S.P. Booth et al., Edinburgh preprint 93/525;  
C. Bernard, Y. Shen and A. Soni, preprint BUHEP/93-13.
- [112] C. Bernard, P. Hsieh and A. Soni, Washington University preprint Wash. U. HEP/93-35 K.C. Bowler et al., Edinburgh preprint 93/528.
- [113] R. Gupta, T. Bhattacharya and D. Daniel, Los Alamos preprint LA UR-93-3580.